CASE FILE
COPY

NACA

RESEARCH MEMORANDUM

INVESTIGATION OF LOCAL HEAT-TRANSFER AND PRESSURE DRAG CHARACTERISTICS OF A YAWED CIRCULAR CYLINDER AT SUPERSONIC SPEEDS

By Glen Goodwin, Marcus O. Creager, and
Ernest L. Winkler

Ames Aeronautical Laboratory
Moffett Field, Calif.

NATIONAL ADVISORY COMMITTEE
FOR AERONAUTICS
WASHINGTON

January 24, 1956
Declassified February 8, 1960

NATIONAL ADVISORY COMMITTEE FOR AERONAUTICS

RESEARCH MEMORANDUM

INVESTIGATION OF LOCAL HEAT-TRANSFER AND PRESSURE DRAG CHARACTERISTICS OF A YAWED CIRCULAR CYLINDER AT SUPERSONIC SPEEDS

By Glen Goodwin, Marcus O. Creager, and
Ernest L. Winkler

SUMMARY

Local heat-transfer coefficients, temperature recovery factors, and pressure distributions were measured on a circular cylinder at a nominal Mach number of 3.9 over a range of free-stream Reynolds numbers from 2.1×10^3 to 6.7×10^3 and yaw angles from 0° to 44°.

It was found that yawing the cylinder reduced the local heat-transfer coefficients, the average heat-transfer coefficients, and the pressure drag coefficients over the front side of the cylinder. For example, at 44° of yaw the average Nusselt number is reduced by 34 percent and the pressure drag by 60 percent. The amount of reduction may be predicted by a theory presented herein. Local temperature recovery factors were also reduced by yaw, but the amount of reduction is small compared to the reduction in heat-transfer coefficients.

A comparison of these data with other data obtained under widely different conditions of body and stream temperature, Mach number, and Reynolds number indicates that these factors have little effect upon the dropoff of heat transfer due to yaw.

INTRODUCTION

Current interest in the flight of aircraft and missiles at high supersonic speeds has brought with it the problem of aerodynamic heating of the aircraft skin and structure. One of the parts of the aircraft where heating is most severe is the leading edge of wings. If these leading edges are sharp and thin, there is little material available to absorb or dissipate the heat. Also, uneven heating of sharp leading edges may result in high thermal stresses.

A method of alleviating this problem is to blunt the leading edges of wings, which reduces the local rate of heat input compared to a sharp leading edge, and provides additional material at the leading edge which gives additional strength and increased thermal capacity.

Blunting the leading edge of a wing normally imposes a drag penalty; however, if the leading edge is swept back, the drag due to the blunted leading edge can be materially reduced. This fact is demonstrated in reference 1 in which drag of a yawed circular cylinder is measured at a Mach number of nearly 7. Another advantage to be gained by sweeping the leading edge is that the heat transfer rate to the leading edge is reduced below that occurring if the leading edge is normal to the direction of flight. This benefit is brought about by a reduction in both the heat-transfer coefficient and the temperature recovery factor. The fact that yawing a circular cylinder reduces the average heat-transfer coefficient has been recognized for years by workers in the field of hot-wire anemometry. King, in 1914, measured this effect (see ref. 2). References 3 and 4 summarize later work in this field. Recently, average heat-transfer rates to yawed and unyawed wires have been measured (ref. 5) and it was found that the reduction of heat transfer by yawing discovered by the workers in the field of hot-wire anemometry persisted at Mach numbers of the order of 10.

Previous experimental work in this field, for the case of supersonic flow over the cylinder, has been limited to measurements of average heat-transfer coefficients or average heat-transfer rates over either the front half of the cylinder or over the entire cylinder. The general purpose of the research described in this paper is to study the effect of yaw upon both the local heat transfer and the pressure drag of a circular cylinder immersed in a supersonic air stream.

The experimental portion of the investigation consisted of measuring local heat-transfer coefficients, local temperature recovery factors, and pressure distribution on a 1-inch-diameter circular cylinder at angles of yaw from 0° to 44°. The tests were conducted in the Ames 8-inch low-density wind tunnel at a nominal Mach number of 3.9 and over a free-stream Reynolds number range of from 2.1×10^{3} to 6.7×10^{3}.

In addition to the experimental portion of the investigation, a theory is derived from which local heat-transfer coefficients and pressure drag coefficients over the front half of a yawed circular cylinder may be predicted to an accuracy sufficient for most engineering purposes.

NOTATION

a speed of sound, ft/sec

C constant in relation $\frac{\mu}{\mu_t} = C \frac{T}{T_t}$

C_D pressure drag coefficient, based on projected area

c_p specific heat of air at constant pressure, ft-lb/slug, $^{\circ}F$

D cylinder diameter, ft

E constant in relation $\frac{k}{k_t} = E \frac{T}{T_t}$

f new variable in momentum equation (5)

$F(\Lambda,M)$ function of yaw angle defined by $\frac{p_{x=0}}{p_{t_2}} \frac{a_{x=0}}{a_t}$

g new variable in energy equation defined by $\frac{i - i_s}{i_t - i_s}$

$G(M)$ function of Mach number defined by $\frac{p_{t_2}}{p_\infty} \frac{a_\infty}{a_t} \frac{1}{M}$

h local heat-transfer coefficient, Btu/ft^2, hr, $^{\circ}F$

i total enthalpy, ft-lb/slug

k thermal conductivity of air, Btu/ft^2, hr, $^{\circ}F$/ft

M Mach number, $\frac{U}{a_\infty}$, dimensionless

Nu Nusselt number, $\frac{hD}{k_t}$, dimensionless

p pressure, lb/ft^2

Pr Prandtl number, $\frac{c_p \mu}{k}$ (consistent units), dimensionless

p_t wind-tunnel reservoir pressure, microns of mercury absolute

q heat-transfer rate, Btu/hr

R_∞ Reynolds number, $\frac{\rho_\infty U D}{\mu_\infty}$, dimensionless

R_2 Reynolds number, $\frac{\rho_\infty UD}{\mu_{t_2}}$, dimensionless

S surface area, ft^2

T temperature, ^oR

T_r local recovery temperature, ^oR

U free-stream velocity ahead of normal shock wave, ft/sec

u,v,w velocity components in x, y, and z directions, respectively, ft/sec

x,y,z coordinates on cylinder, ft

β constant of proportionality between velocity u_1 and surface coordinate x defined by relation $u_1 = \beta x$

γ ratio of specific heats, dimensionless

μ viscosity of air, lb-sec/ft^2

ρ density of air, slugs/cu ft

ν kinematic viscosity, ft^2/sec

η new variable in momentum equation defined by $\left(\frac{\beta}{\nu}\right)^{1/2} z$

η_r temperature recovery factor, $\frac{T_r - T_\infty}{T_t - T_\infty}$, dimensionless

Λ angle of yaw, deg

φ azimuth angle measured from forward stagnation point, degrees or radians as noted

$\Phi(\varphi)$ function of azimuth angle defined by $\frac{p_1}{p_{x=0}}$

Subscripts

s surface of body

1 conditions at outer edge of boundary layer

2 conditions just downstream of normal shock wave

t total conditions (i.e., conditions that would exist if the gas were brought to rest isentropically)

av average quantity over front half of cylinder

∞ free-stream conditions ahead of shock wave from cylinder

ANALYSIS

Before proceeding with the details of the analysis, the main purposes will be outlined. Briefly, it was hoped that the theory would yield, as a minimum result, correlation parameters or dimensionless groupings which could be used to correlate the experimental data, and, secondly, that the functional relationships between the local Nusselt number and these parameters could be deduced. As an additional objective, it was hoped that the theory would provide a means by which Nusselt numbers could be predicted at flow conditions different from those at which tests have been conducted. The degree to which these objectives have been realized is discussed in later sections.

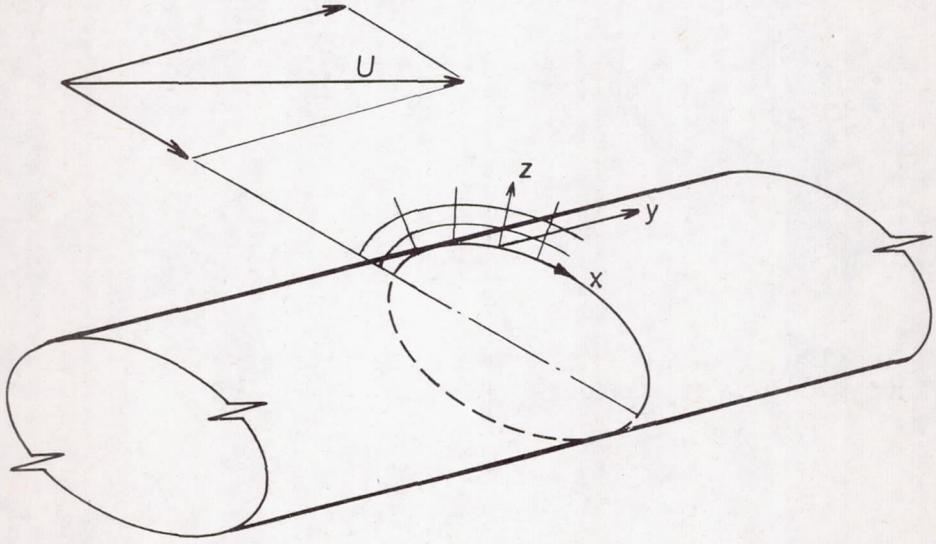

Sketch (a)

By means of order of magnitude arguments similar to those used by Sears (ref. 6) the momentum, continuity, and energy equations for laminar flow over an infinite yawed cylinder can be developed.[1] In a coordinate system (see sketch (a)) where x is measured along the surface of the

[1]Crabtree (ref. 7) obtains the same set of equations in a recently published work.

cylinder from the stagnation point in a direction perpendicular to the axis, z measured normal to surface and y measured spanwise, the conservation of momentum in the x direction is given by

$$\rho u \frac{\partial u}{\partial x} + \rho w \frac{\partial u}{\partial z} = - \frac{\partial p}{\partial x} + \frac{\partial}{\partial z}\left(\mu \frac{\partial u}{\partial z}\right) \tag{1}$$

Conservation of momentum in y direction reduces to

$$\rho u \frac{\partial v}{\partial x} + \rho w \frac{\partial v}{\partial z} = \frac{\partial}{\partial z}\left(\mu \frac{\partial v}{\partial z}\right) \tag{2}$$

The equation of continuity of mass is given by

$$\frac{\partial}{\partial x}(\rho u) + \frac{\partial}{\partial z}(\rho w) = 0 \tag{3}$$

The conservation of total energy for a Prandtl number of 1 is given by

$$\rho u \frac{\partial i}{\partial x} + \rho w \frac{\partial i}{\partial z} = \frac{\partial}{\partial z}\left(\mu \frac{\partial i}{\partial z}\right) \tag{4}$$

where

$$i = \frac{u^2 + v^2}{2} + c_p T$$

If the flow is assumed incompressible with constant properties and the following change of variables is made

$$u = \beta x f_\eta(\eta)$$

$$w = -(\nu\beta_\eta)^{1/2} f(\eta)$$

$$u_1 = \beta x$$

$$g(\eta) = \frac{i - i_s}{i_t - i_s}$$

$$\eta = \left(\frac{\beta}{\nu}\right)^{1/2} z$$

the momentum equation in the x direction transforms to (see, e.g., ref. 8)

$$f_\eta^2 - ff_{\eta\eta} = 1 + f_{\eta\eta\eta} \tag{5}$$

and the energy equation transforms to

$$g_{\eta\eta} + fg_\eta = 0 \tag{6}$$

where the subscript η denotes differentiation with respect to the new variable η. These transformations are given in detail in reference 8.

The enthalpy variable $g(\eta)$ is taken to be a function of η only and has the limits $g(\eta) = 1$ at $\eta = \infty$ and $g(\eta) = 0$ at $\eta = 0$. It can be shown that $\partial g(\eta)/\partial x$ is a term of small order in comparison to the term $\partial g(\eta)/\partial \eta$ if the approximations made to derive equations (1), (2), and (4) from the more general Navier-Stokes and energy equation hold.

The heat-transfer rate per unit area is given by the solution of equations (5) and (6) and is

$$\frac{q}{S} = k(T_t - T_s)\left(\frac{\beta}{\nu}\right)^{1/2}(g_\eta)_s \tag{7}$$

where

$$(g_\eta)_s = 0.570$$

The solution to equations (5) and (6) were obtained by Pohlhausen in 1921 (see ref. 8).

If the heat-transfer coefficient is defined by

$$h = \frac{q/S}{T_t - T_s} \tag{8}$$

then

$$h = 0.570\ k\left(\frac{\beta}{\nu}\right)^{1/2} \tag{9}$$

The above equation (9) gives no hint as to where in the boundary layer the kinematic viscosity and thermal conductivity should be evaluated; however, there are various pieces of evidence to guide the choice. One method, widely used (see, e.g., ref. 9), is to assume a linear relationship between viscosity and temperature and between thermal conductivity and temperature, and to evaluate the pressure at the outer edge of the

boundary layer (since $\partial p/\partial z$ has been assumed equal to 0 in the boundary layer). The constant β was evaluated from pressure distribution data and will be discussed in a later section. Cohen and Reshotko (ref. 10) discuss the effect of Prandtl number on the heat-transfer coefficient. They found that the factor $Pr^{0.4}$ multiplied times the heat-transfer coefficient obtained from the analysis where the Prandtl number is assumed equal to 1 accounts for this effect. This factor is included in the following equation (10a). The above assumptions yield, if $\beta = 2.13 \frac{a_{x=o}}{D}$

$$h = 0.588 \frac{E}{\sqrt{C}} Pr^{0.4} k_t \sqrt{\frac{\rho_{t_2} a_t}{\mu_t \frac{D}{2}}} \left(\frac{p_1}{p_{x=o}}\right)^{1/2} \left(\frac{p_{x=o}}{p_{t_2}}\right)^{1/2} \left(\frac{a_{x=o}}{a_t}\right)^{1/2} \tag{10a}$$

where

$$\frac{p_1}{p_{x=o}} = \left[1 - \frac{\gamma - 1}{2}\left(2.13 \frac{x}{D}\right)^2\right]^{\frac{\gamma}{\gamma-1}} \tag{10b}$$

$$\frac{p_{x=o}}{p_{t_2}} = \cos^2\Lambda + \left[\frac{\left(\frac{2\gamma M^2}{\gamma + 1} - \frac{\gamma - 1}{\gamma + 1}\right)^{\frac{1}{\gamma-1}}}{\left(\frac{\gamma + 1}{2} M^2\right)^{\frac{\gamma}{\gamma-1}}}\right] \sin^2\Lambda \tag{10c}$$

$$\frac{a_{x=o}}{a_t} = \left(1 - \frac{\frac{\gamma - 1}{2} M^2 \sin^2\Lambda}{1 + \frac{\gamma - 1}{2} M^2}\right)^{1/2} \tag{10d}$$

From equation (10), the effect of yaw angle Λ upon the heat-transfer coefficient at the forward stagnation point is given by

$$\frac{h_\Lambda}{h_{\Lambda=o}} = \left(\frac{p_{x=o}}{p_{t_2}}\right)^{1/2} \left(\frac{a_{x=o}}{a_t}\right)^{1/2} \tag{11}$$

Also from equation (10) the effect of azimuth angle φ upon the ratio of the local heat-transfer coefficients is given by

$$\frac{h_\varphi}{h_{\varphi=0}} = \left(\frac{p_1}{p_{x=0}}\right)^{1/2} \tag{12}$$

DESCRIPTION OF EQUIPMENT AND EXPERIMENTAL METHOD

Wind Tunnel

The tests were conducted in the Ames 8-inch low-density wind tunnel. This wind tunnel is an open-jet nonreturn type tunnel. Air was used as the test gas. The 8-inch tunnel is a scaled up version of the low-density wind tunnel described in reference 11. A five-stage set of steam ejectors is used to produce the main flow. The axisymmetric nozzle was designed by the method described in reference 12, with the additional feature of boundary-layer removal. The nozzle was constructed of shim stock of varying thickness and alternate shims were removed to permit boundary-layer removal as described in reference 13. The design Mach number was 4 through the stream-static pressure range of 100 to 400 microns of mercury. The boundary layer is removed by a set of steam ejectors operating in parallel with the main drive ejector set. The physical arrangement of the nozzle and test section is shown in figure 1.

Preliminary surveys of the nozzle indicated that no strong shock waves were present in the nozzle when the expansion ratio across it was properly set and controlled. The air stream was surveyed with an open-end impact pressure probe. Surveys were made in a plane normal to the stream direction 1-1/4 inches downstream of the nozzle exit. Surveys were also made in the nozzle along the stream center line. The static pressure of the stream was obtained by measuring the nozzle wall pressure at a point 2 inches upstream of the exit plane of the nozzle. This method of obtaining stream static pressure has been described in reference 12.

A typical Mach number distribution obtained from these measured quantities is shown in figure 2. The Mach number was calculated in two ways, (1) from measured impact pressure and static (wall tap) pressure together with the assumption of a normal shock wave standing ahead of the impact pressure probe and isentropic deceleration of the flow behind the shock wave (circular points) and (2) from measured impact pressure and upstream reservoir pressure (total head) using the assumption that the flow through the nozzle was isentropic (shown by the square symbols). Good agreement was obtained between the two methods of obtaining Mach number over the range of pressure levels used in the investigation. Therefore the assumption that the flow through the nozzle was isentropic (in the test region) appears to be reasonable.

Table I presents the actual usable stream diameter and Mach number obtained for various test section static pressures.

Model

The heat-transfer model was a 6-inch-long cylindrical copper shell of 1-inch outside diameter and 1/4-inch-thick wall (see fig. 3). A copper plug, 1/8-inch diameter and 1/8-inch long, was inserted into a hole in this shell, with a 1/64-inch air gap between the plug and the shell. The surface of the plug was machined to the contour of the cylinder. The body (or shell) was instrumented with an electrical heater at each end spaced 2-1/2 inches from the plug, a thermocouple embedded in the shell under each end heater, and a thermocouple in the shell near the plug. An electrical heating coil was wound on the plug, and a differential thermocouple mounted between the plug and the shell. This differential thermocouple was used to indicate the temperature difference between the plug and the shell. Mechanical means located outside of the stream were provided in the mounting to permit rotation and yaw of the cylinder which completely spanned the stream.

A plastic film, 0.00025-inch thick, was wrapped around the cylinder to seal the air gap between the plug and the body shell. The air gap was then vented to the hollow portion of the cylinder and thence to the constant static pressure of the test section. Thus the heat loss due to conduction through the air gap is reduced as much as possible because of the presence of a quiescent layer of low pressure air around the test plug.

The pressure model was constructed from a 1-inch diameter cylindrical shell. A pressure tap of 0.035-inch diameter was located in the center of the cylinder, the pressure at the tap was measured by an oil-filled U-tube manometer. Pressures were measured for various azimuth positions around the cylinder at 0°, 30°, 45°, and 60° of yaw.

Test Method

The heat transferred from the surface of the plug to the air stream was determined as a function of the difference between the plug temperature and the stream stagnation temperature. A test point was obtained by heating the cylinder and the test plug to the same constant temperature, and measuring the plug heater current for this steady-state condition. A series of tests were made with no air flow through the tunnel at approximately 0.1 micron and at pressures of 100 to 300 microns, to obtain the radiation and conduction loss. The variation of these losses with pressure was within the experimental scatter of the tare data. These heat losses were then treated as a tare loss to be subtracted from the gross heat input to the plug obtained in the tests. The magnitude of the tares was found to be approximately 10 percent of total heat input at highest rates, and approximately 60 percent of total heat input at the lowest rates present on the back side of the cylinder. At a given orientation

of the local test spot, net heat input to the plug was obtained at a series of plug temperature levels, ranging from 20° to 50° Fahrenheit above stagnation temperature. This net heat into the plug, which is then the heat transported from the plug to the stream, was plotted as a function of the difference between plug temperature and stagnation temperature. The slope of this curve is proportional to the product of the heat-transfer coefficient and the test area which was taken slightly larger than the plug area as explained in Appendix A. Extrapolation of the curve to zero heat transported gives an intercept which is the difference between recovery temperature and stagnation temperature. A typical test curve is shown in figure 4. Similar experimental curves were obtained at azimuth angles of 0° to 90°, at yaw angles of 0°, 30°, and 44°, and for stagnation temperature of 520° R. At zero angle of yaw, these curves were obtained up to azimuth angles of 180° at one test condition.

Tests were performed on a different body to determine the effect of the thickness of the Mylar film covering the plug. Both tare tests and heat-transfer tests were made using two different thicknesses of Mylar film. The effect of the additional layer of film on the results was within the scatter of the data.

RESULTS AND DISCUSSION

Experimental Results

The experimentally determined local heat-transfer coefficients plotted versus azimuth angle for the case of the cylinder normal to the stream are shown in figure 5. The solid lines are faired through the experimental points obtained over a range of free-stream Reynolds number. It can be seen that heat-transfer coefficients decrease monotonically back to an azimuth angle of 90°. Over the rear portion of the cylinder, the heat-transfer coefficients are very low compared to the value at the stagnation point; the average value being only about 11 percent of its value at the stagnation point.[2] It can be seen that lowering the Reynolds number of the flow decreases the local heat-transfer coefficients over the front half of the cylinder as is also the case in subsonic flow.

In order to calculate the actual local heat-transfer rates from the cylinder, the local recovery temperature must be known. Local free-stream temperature recovery factors are shown in figure 6 for the same conditions

[2]The accuracy of the measurement on the rear portion is reduced due to low heat-transfer coefficients and relatively high tares (approximately 60 percent of total heat input). It may be of interest to point out here that the pressures measured on the back side of the cylinder were very low, as may be seen from the data tabulated in table II.

of flow given in figure 5. It can be seen that the temperature recovery factor decreases from a value of unity at the forward stagnation point to a value of 0.67 at an azimuth angle of 120° and then increases toward unity as the rearward stagnation point is approached.[3] Also changing the Reynolds number of the flow did not appear to materially alter the variation of local temperature recovery factor over the front half of the cylinder.

Other investigators have measured local temperature recovery factors on cylinders normal to the stream and the results of these tests are summarized in reference 14. Up to an azimuth angle of 60° the data of this reference agreed well with the results of the present tests, as can be seen in figure 6. At azimuth angles between 60° and 150° the present tests give results which are much lower than those of reference 14. For azimuth angles between 150° and 180°, the results of the present tests are higher than those of reference 14. In the experiments described in this reference, sharp changes in recovery temperature would tend to average out due to heat conduction in the models.

This dropping-off of recovery factor with azimuth angle tends to make the front portion of the cylinder even more controlling of the heat rates than would be indicated by the ratios of heat-transfer coefficients at the 90° point to those at the forward stagnation point. A statement of the amount of heat transferred from the front half compared to that transferred by the back half is difficult if not impossible to make unless the stagnation temperature of the flow and wall temperatures of the body are specified, as the heat-transfer rates depend upon the heat-transfer coefficient and the driving temperature potential for all cases where the wall temperature is not very small compared to the stream stagnation temperature.

The effect of sweep or yaw angle upon local heat-transfer coefficients is shown parametrically in figure 7 wherein the local heat-transfer coefficient is shown versus azimuth angle for a free-stream Reynolds number of 6.7×10^3. Three angles of sweep are shown, 0°, 30°, and 44°, and it can be seen that yawing the cylinder reduces the local heat-transfer coefficients at all azimuth angles up to 90°. It is interesting to note that yawing the cylinder reduces the heat-transfer coefficient at any given azimuth angle by approximately the same percentage.

As companion information with figure 7, the local temperature recovery factors at the aforementioned angles of yaw are shown in figure 8 as a function of the azimuth angle. It can be seen from figure 8 that yawing the cylinder reduces the temperature recovery factors. The reduction in recovery factor is, however, small compared to the reduction in heat-transfer coefficient produced by yawing the cylinder. The heat-transfer data are tabulated in table III.

---

[3]See footnote 2, p. 11.

Comparison of Experimental Results and Analysis

Pressure distribution and drag.- Three major assumptions had to be made in the analysis in order to simplify the basic differential equations governing the flow sufficiently to allow a solution. These assumptions were that the Prandtl number was equal to 1, that the flow was incompressible and properties were constant, and that the x component of the external velocity over the front half of the cylinder could be expressed as $u_1 = \beta x$.

The net result of the assumption of $Pr = 1$ is that the analysis yields a recovery factor of 1 or that the recovery temperature of the cylinder is constant and equal to the stream stagnation temperature. That this is not the case can be seen from the data in figures 6 and 8. A similar difficulty arises when this assumption is made in analysis of flow over flat plates. Experience has shown, for the case of flow over flat plates, that the assumption of $Pr = 1$ causes the calculated Nusselt number to be higher than the experimental value by a constant factor equal to $Pr^{1/3}$. When the theoretical value of the Nusselt number, obtained by assuming $Pr = 1$, is used to calculate the actual heat-transfer rate from a flat plate it must be multiplied by $Pr^{1/3}$ and the experimental value of the recovery temperature must be used in the temperature potential in order to obtain results that are in agreement with theory. Cohen and Reshotko (ref. 10) discuss the factor $Pr^{0.4}$ used to correct the theoretical Nusselt number, obtained by assuming $Pr = 1$, for unyawed two-dimensional bodies. The assumption is made here that this factor applies to the yawed cylinder as well.

The assumption that the flow was incompressible and that properties were constant is probably the weakest assumption made in the analysis. However, in the application of the analysis the viscosity is allowed to vary linearly with temperature, and pressure is evaluated at the point on the surface being considered. Comparison of the results of the analysis with experiment will be made in a later section to check the validity of this assumption.

The assumption that the x component of the external velocity over the front half of the cylinder is a linear function of x was checked in the following way. The velocity over the cylinder in the x direction was calculated from measured pressure distribution using Bernoulli's equation for a compressible gas and assuming the fluid velocity was zero at the stagnation point. When this was done it was found that if the constant β was set equal to $2.13\ a_{x=0}/D$ the velocity over the cylinder, yawed or unyawed, could be calculated with good accuracy. By substituting this expression into Bernoulli's equation, the pressure distribution over the front half of the cylinder could be calculated. Figure 9 shows the ratio of the pressure at any azimuth angle to that at the forward stagnation point plotted versus azimuth angle. It can be seen from figure 9 that, for the case of a cylinder normal to the stream, variation in Reynolds number from 6.7×10^3 to 1.4×10^5 and variation in Mach number

from 2.48 to 6.86 does not appreciably alter the pressure ratio distribution over the front half of the cylinder. The solid line was obtained by substituting $u_1 = \beta x$ into Bernoulli's equation and is given by

$$\frac{p_1}{p_{x=o}} = \left[1 - \frac{\gamma - 1}{2}\left(2.13\,\frac{x}{D}\right)^2\right]^{\frac{\gamma}{\gamma-1}} \tag{13}$$

Figure 10 shows the same parameters as figure 9; however, the test points were obtained at yaw angles from 0° to 60°. The solid line is again the curve calculated from equation (13). Although yawing the cylinder does change the pressure over it, from figure 10 it can be seen that the pressure ratio variation is not changed for yaw angle of 0° to 30° in the present tests and 0° to 60° in the tests of reference 1. The pressure distribution over the cylinder measured at 45° and 60° of yaw in the present tests departed from that reported in reference 1 for azimuth angles greater than about 45°. It is suspected that this departure is brought about by the fact that the flow over the cylinder was becoming three-dimensional due to the 1-inch-diameter model in the 3-inch-diameter stream. The conclusion can then be drawn that over the range of variables investigated ($R = 6.7\times10^3$ to 1.4×10^5, $M = 2.48$ to 6.86) that the pressure ratio distribution is a unique function of the azimuth angle for yaw angles of 0° to 30° for the present tests and 0° to 60° for the tests of reference 1. Thus, the assumption of $u_1 = \beta x$ appears to be a reasonable one.

One other assumption must be investigated before the results of the analysis are compared with the experimentally determined heat-transfer results, namely, that the pressure at $x = 0$ on a yawed cylinder may be computed by Rayliegh's equation using the component of the Mach number normal to the cylinder. Figure 11 shows the ratio of the pressure at $x = 0$ to the stream impact pressure plotted versus the yaw angle of the cylinder. The curves were calculated for three Mach numbers using the above-mentioned assumption and the test points are from the present tests and from reference 1. The good agreement between the curves calculated by equation (10c) and the test points indicate that this assumption is also a reasonable one.

The pressure distribution over the front side of a yawed or unyawed cylinder can now be used to compute the effect of yaw upon the pressure drag over the front side of the cylinder. The resultant expression is

$$\frac{(C_D)_\Lambda}{(C_D)_{\Lambda=o}} = \frac{p_{x=o}}{p_{t_2}} \cos \Lambda \tag{14}$$

Figure 12 shows this ratio plotted as a function of the angle of yaw of the cylinder for two Mach numbers. The curves are obtained from equation (14) and the test points shown are from the present tests and from reference 1. The agreement between equation (14) and the experimental points is good. This figure points up the previously mentioned fact that rounding the leading edge of a wing may not lead to severe drag

penalties if the wing is swept. For example, at 45° of sweep the drag coefficient of the swept leading edge is only about 40 percent of its unswept value. Also, the drag coefficient ratio of equation (14) approaches $\cos^3\lambda$ for Mach numbers approaching infinity, which corresponds to Newtonian flow results.

Local Nusselt number.- The ratio of the local Nusselt number or local heat-transfer coefficient to that at the stagnation point is plotted versus azimuth angle in figure 13. Included in this figure are data for three Reynolds numbers and three angles of yaw, 0°, 30°, and 44°. It can be seen that in general the heat-transfer coefficient decreases with azimuth angle. Except for the data taken at 44° of yaw, all of the points tend to form a single curve. This fact tends to substantiate the result of the analysis which shows that this ratio is a function of azimuth angle only. The variation of heat-transfer coefficient ratio given by the analysis is shown as the solid curve and was calculated from the expression

$$\frac{h_\varphi}{h_{\varphi=0}} = \left(\frac{p_1}{p_{x=0}}\right)^{1/2} \tag{15}$$

It can be seen that at the lower azimuth angles the analysis fits the data reasonably well, but at the azimuth angles of 60° and 75° the theory predicts values larger than those observed experimentally.

At an azimuth angle of 60° the Mach number at the edge of the boundary layer has reached a value of about 1.2 and at the 75° point the Mach number is 1.65.

In order to determine if compressibility was responsible for the dropoff of the measured values of heat transfer below those given by the analysis for these azimuth angles, the theory of Cohen and Reshotko, reference 15, was compared with the data for the case of zero yaw. This theory, which accounts for the effects of compressibility but not for the effects of yaw, is shown by the dashed curves. It is apparent that the theory fits the data better at these higher azimuth angles than the incompressible one. However, if average values of the Nusselt number are considered, the difference between the compressible and the incompressible theory is a constant, and because of the uniqueness of the Mach number distribution over the front half of the cylinder, the incompressible theory may be used to correlate data over a wide range of Mach numbers.

The result of the present analysis (eq. (10)) may be written in terms of the local Nusselt number, Prandtl number, Reynolds number evaluated behind the bow shock wave, a function of the free-stream Mach number, a function of the azimuth angle, and a function of both the yaw angle and the free-stream Mach number. The local Nusselt number is then given by

$$Nu_{local} = \frac{hD}{k_t} = 0.832\ Pr^{0.4}\sqrt{R_2}\sqrt{F(\Lambda,M)G(M)\Phi(\varphi)} \tag{16}$$

where

$$F(\Lambda,M) = \left(\frac{p_{x=o}}{p_{t_2}}\right)\left(\frac{a_{x=o}}{a_t}\right)$$

$$G(M) = \left(\frac{p_{t_2}}{p_\infty}\right)\left(\frac{a_\infty}{a_t}\right)\left(\frac{1}{M}\right)$$

$$\Phi(\varphi) = \frac{p_1}{p_{x=o}}$$

Equation (16) is compared with the data on a local basis in figure 14 where the local Nusselt number is shown plotted versus the parameter $R_2F(\Lambda,M)G(M)\Phi(\varphi)$. The result of the analysis is shown as the solid curve and the test points shown are for three Reynolds numbers, angles of yaw from 0° to 44°, and azimuth angles from 0° to 60°. The data are correlated by the analysis to within a mean deviation of 10 percent.

Average Nusselt number.- The result of the analysis is compared with the experimental data in figure 15 whereon the average Nusselt number for the front half of the cylinder is plotted versus the dimensionless parameter $R_2F(\Lambda,M)G(M)$. The solid line is the result of the analysis and is given by the following expression which was obtained by integrating $\Phi(\varphi)$ over the front half of the cylinder

$$Nu_{av} = 0.5935\ Pr^{0.4}\sqrt{R_2}\ [F(\Lambda,M)G(M)]^{1/2} \tag{17}$$

where Nu_{av} and R_2 are evaluated using free-stream density and velocity but viscosity and conductivity evaluated at stagnation conditions.

The experimental points in the figure (solid points) were obtained during the present investigation at three Reynolds numbers and at angles of yaw of 0°, 30°, and 44°.

The agreement between the calculated and experimental values of average Nusselt number over the front half of the cylinder is within ±10 percent for all points except the value obtained at zero angle of yaw at the lowest Reynolds number ($R_2 = 610$). This point is 15 percent below the predicted curve.

Also shown in figure 15 are average Nusselt numbers for the front half of yawed and unyawed cylinders obtained in the 11-inch wind tunnel at Langley Field, reference 16, at a Mach number of 6.9 and at free-stream Reynolds numbers of 1.3×10^5 and 1.8×10^5. The yaw angle was varied from 0° to 75° in these tests. It can be seen that the results of the analysis correlate the Mach number 6.9 data reasonably well up to angles of yaw of

60°. At an angle of yaw of 75° the data of reference 16 do not correlate well with the result of the analysis. It is stated in reference 16 that the data taken at 75° of yaw may not be reliable due to model limitations. This effect is attributed to lack of two-dimensionality at the high yaw angle. The data of reference 16 were obtained with heat flow into the model at a stagnation temperature of 1140° R and over a range of model temperatures from 570° R to 910° R. The present data were obtained with heat flow out of a model at a stagnation temperature of 520° R and model temperatures of 540° R to 570° R. No effect on the heat-transfer results could be detected under these widely different conditions.

The effect of yaw upon the average Nusselt number over the front half of the cylinder can best be shown in the next figure (fig. 16) where the ratio of Nusselt number obtained at yaw to that obtained at zero yaw is plotted as a function of the angle of yaw. Also shown in this figure are data from reference 16. It can be seen that yawing a cylinder reduces the average Nusselt number over that obtained at zero yaw. At 30° of yaw the reduction shown by the present data is approximately 16 percent and at 44°, 33 percent of the zero yaw value. The curves shown in the figure are the result of the analysis and were calculated from the following expression

$$\frac{h_\Lambda}{h_{\Lambda=0}} = \frac{(Nu_{av})_\Lambda}{(Nu_{av})_{\Lambda=0}} = [F(\Lambda,M)]^{1/2} \tag{18}$$

for three Mach numbers, 4, 7, and ∞. It can be seen that $F(\Lambda,M)$ is a weak function of the free-stream Mach number at yaw angles less than about 45° but for large yaw angles the theory predicts a sizeable effect of Mach number on $\frac{h_\Lambda}{h_{\Lambda=0}}$. The data and the predicted result are in good agreement up to angles of yaw of 44°. At an angle of yaw of 60° and 75°, the data of reference 16 lie above the predicted curve.

An effort was made in the present investigation to extend the range of the tests to an angle of yaw of 60°; however, an examination of the pressure distribution over the model at this yaw angle (see fig. 10) disclosed a departure from that obtained at the lower yaw angles. At the lower yaw angles, namely 30°, an examination of figure 10 reveals that the pressure distribution over the cylinder agreed very well with that reported in reference 1 where the flow was shown to be two-dimensional. It is suspected that the deviation at 44° and 60° yaw angles was due to the flow over the cylinder becoming three-dimensional because of the relatively large model (1-inch diameter) in the 3-inch-diameter stream.

Heat-transfer results obtained at 60° of yaw also exhibited large scatter (about 37-percent maximum spread) and an examination of the model revealed that small air bubbles were present between the measuring plug and the plastic film. Also electrical shorts between the cylinder test

body and the plug heater wires developed about this time. For these reasons the data obtained at 60° of yaw were considered unreliable and are not included.

Application to Flight Conditions

The results, obtained during the present investigation, were for the case where the body temperature was very nearly the stream stagnation temperature. At high Mach number (5 or above) the stagnation temperature obtained during flight may be so high that the aircraft or missile must be cooled to a temperature much below the stream stagnation temperature. It is of interest, then, to compare the results of these tests and this analysis with any data which are available that approximate (as far as temperature is concerned) flight conditions. The results reported in reference 5 were obtained at a Mach number of 9.8, a stream stagnation temperature of 2200° R and a test body temperature of 520° R. The tests were conducted on small wires (0.003- to 0.020-inch diameter) at angles of yaw up to 70°.

Even though the tests of reference 5 were conducted at a relatively low Reynolds number (315 for the 0.003-inch wire), the data when compared with the present tests should indicate in a limited way whether the results of the present tests may be applied to the case of a cool body in a hot hypersonic air stream. In reference 5 the recovery temperature could not be measured; therefore, comparison will have to be made by applying the results of the present tests to the specific conditions under which the experiments reported in reference 5 were made. The results reported in reference 5 were for heat transfer from the entire cylinder, whereas the present tests are for the front side of the cylinder only. During one run in the present tests the local heat transfer on the back side of the cylinder for the zero yaw condition was obtained. These results are shown in figure 7 and it can be seen that the heat-transfer coefficients on the back side of the cylinder were low, being only about 10 percent of the value at the stagnation point. In the comparison shown in figure 17 it was assumed that the heat transfer from the back side of the cylinder reported in reference 5 could be neglected.

Figure 17 shows such a comparison whereon the ratio of total heat-transfer rate at angle of yaw to that obtained at zero angle of yaw is plotted versus angle of yaw. The circled symbols are from reference 5 and the square symbols are the results of the present tests applied to the above-mentioned stream conditions. The agreement between the two sets of data is good, and within the scatter of the data there again appears to be no effect of temperature potential upon the dropoff of heat transfer with yaw. The solid line is obtained from equation (18) with the assumption of constant temperature recovery factor equal to 1.

CONCLUSIONS

The following general conclusions are drawn from the results of this investigation:

1. Local heat-transfer coefficients, average heat-transfer coefficients, and pressure drag coefficients for the front side of a circular cylinder are reduced by yawing the cylinder as found by other investigators. For example, at 44° of yaw the average Nusselt number is reduced by 34 percent and the pressure drag by 60 percent. The amount of the reduction may be predicted with sufficient accuracy for most engineering purposes by a theory presented herein.

2. Local temperature recovery factors on the front side of a cylinder are reduced by yaw. But this effect is small compared to the reduction in heat-transfer coefficients.

3. A comparison of these data obtained with body temperature near stream stagnation temperature with other data obtained with a varying body temperature in a hot hypersonic air stream indicates that these widely different temperature conditions have little effect upon the dropoff of heat transfer due to yaw.

4. The heat-transfer coefficients on the back side of a cylinder normal to the stream were insignificant compared to those on the front side for $M = 3.9$ and a free-stream Reynolds number of 6.7×10^{3}.

Ames Aeronautical Laboratory
National Advisory Committee for Aeronautics
Moffett Field, Calif., Aug. 31, 1955

APPENDIX A

DETERMINATION OF THE HEAT-TRANSFER AREA

The net heat was considered to be transferred from the top surface of the cylindrical test plug to the air stream. Thus, the area, S, used in the following heat-transfer rate equation, was the area of the top of the test plug.

$$q = hS(T - T_r) \tag{A1}$$

However, the film stretched over the model (see fig. 3 insert) does conduct some heat away from the plug. Also, the film receives energy from the cylindrical surface of the plug by free molecular conduction through the annular air space around the plug. This film acts much as a circular fin in dissipating the heat from the test plug and hence it is necessary to increase the area to be used in calculating the heat-transfer coefficient. The following analysis of the fin effect leads to a determination of the correction to the test area.

The differential equation governing the temperature distribution in the circular-film fin may be found by summing the quantities of heat transferred by the various means to and from a circular element of the fin. Azimuth variations of these quantities around the test plug will be considered negligible. The assumption is made that temperature differences are small, so that the radiation exchange terms may be written in linear form. The width of the annular air space is of the order of a mean-free-path length of the gas; thus, it is assumed that the circular element of fin gains heat from the plug by free molecular conduction through the annular air space. The elemental fin also transfers heat to the stream by convection through the flow boundary layer. A further assumption will be made that the variation of heat-transfer coefficient and recovery temperature is negligible over the area of film considered. On the basis of these assumptions and with normal conduction in the film fin, the differential equation is found to be,

$$\frac{d^2\left(T - \frac{A}{B}\right)}{dr^2} + \frac{1}{r}\frac{d\left(T - \frac{A}{B}\right)}{dr} - B\left(T - \frac{A}{B}\right) = 0 \tag{A2}$$

where

T temperature along the fin radius

r radial distance from center of plug

and the constants are defined by

$$A = \frac{T_p}{tk_f}\left(\frac{3NV_m\kappa}{2\sqrt{\pi}} + 4\sigma\epsilon T_o^3\frac{T_o}{T_p} + h\frac{T_r}{T_p}\right) \tag{A3}$$

$$B = \frac{1}{tk_f}\left(\frac{3NV_m\kappa}{2\sqrt{\pi}} + 4\sigma\epsilon T_o^3 + h\right) \tag{A4}$$

and

k_f thermal conductivity of film, Btu/hr ft^2 $^\circ$F/ft

t thickness of film, ft

N number of molecules per unit volume, 1/ft^3

V_m most probable molecular speed, ft/sec

κ Boltzmann constant, 7.27×10^{-27} Btu/molecule $^\circ$F

σ Stefan-Boltzmann constant, 4.8×10^{13} Btu/ft^2 sec $^\circ$R^4

ϵ emissivity, dimensionless

T_p temperature of plug, $^\circ$R

T_o temperature of surrounding surfaces, $^\circ$R

This differential equation (A2) is a form of Bessel's equation. The solution may be written in terms of modified Bessel functions of zero order, first and second kinds, as

$$T - \frac{A}{B} = A_3 I_o(r\sqrt{B}) + A_4 K_o(r\sqrt{B}) \tag{A5}$$

where A_3 and A_4 are constants of integration to be determined by the following boundary conditions,

$$\left.\begin{aligned} r &= r_p,\ T = T_p \\ r &= r_B,\ T = T_p \\ r &= r_m,\ \frac{dT}{dr} = 0 \end{aligned}\right\} \tag{A6}$$

where

r_p radius of plug, ft

r_B outer radius of annular space around plug, ft

r_m radius at which minimum temperature occurs on fin, ft

Since the value of r_m is not known, the three boundary conditions (A6) determine r_m as well as the two constants of integration.

In the range of interest, the modified Bessel functions in the solution (A5) may be replaced by the asymptotic expressions (ref. 17) for large values of the argument $r\sqrt{B}$. These expressions are

$$\left.\begin{aligned} I_0(r\sqrt{B}) &\cong \frac{\exp(r\sqrt{B})}{\sqrt{2\pi r\sqrt{B}}} \\ K_0(r\sqrt{B}) &\cong \sqrt{\frac{\pi}{2r\sqrt{B}}}\ \exp(-r\sqrt{B}) \end{aligned}\right\} \tag{A7}$$

We introduce relations (A7) into equation (A5), apply the boundary conditions, and evaluate the constants of integration. The radius, r_m, at which the minimum temperature occurs is found to be very nearly the average radius given by

$$r_m = \frac{r_B + r_p}{2} \tag{A8}$$

The temperature distribution in the circular fin is then given by the resulting form of equation (A5) as

$$\frac{T - \frac{A}{B}}{T_p - \frac{A}{B}} = \sqrt{\frac{r_p}{r}}\left[\frac{\exp(r\sqrt{B}) + \left(\frac{2r_m\sqrt{B}-1}{2r_m\sqrt{B}+1}\right)\exp(2r_m\sqrt{B} - r\sqrt{B})}{\exp(r_p\sqrt{B}) + \left(\frac{2r_m\sqrt{B}-1}{2r_m\sqrt{B}+1}\right)\exp(2r_m\sqrt{B} - r_p\sqrt{B})}\right] \tag{A9}$$

The heat removed from the plug by the film is transferred to the stream according to the following relation

$$dq = h(T - T_r)dS \tag{A10}$$

This expression is integrated using the temperature distribution found in equation (A9) for T and assuming a constant heat-transfer coefficient. The resulting expression is

$$q = 2\pi h \int_{r_p}^{r_m} (T - T_r) r \, dr \tag{A11}$$

If we assume that the amount of heat represented in equation (A11) were to be transferred at plug temperature from an area given by an equivalent radius, $\bar{r}$, we have

$$q = 2\pi h(\bar{r}^2 - r_p^2) \tag{A12}$$

Thus by equating the right-hand sides of equations (A11) and (A12) we can express the heat-transfer radius $\bar{r}$ as follows:

$$\bar{r}^2 = r_p^2 + \frac{r_p^2}{\left(1 - \frac{T_r}{T_p}\right)} \left[2\int_1^{\frac{r_m}{r_p}} \left(\frac{r}{r_p}\right)\left(\frac{T}{T_p}\right) d\left(\frac{r}{r_p}\right) - \frac{T_r}{T_p}\left(\frac{r_m^2}{r_p^2} - 1\right) \right] \tag{A13}$$

In actual computation of the correction, the emissivity of the film was taken to be 0.1 (i.e., that of the chrome-plated plug surface). The emissivity of the plug with film was found to check closely with the value normally taken for polished chrome. The conductivity of the film was taken as 0.1 Btu/hr ft^2 $^\circ$F/ft. This value was obtained from the manufacturer's literature, and was not checked experimentally during these tests. The first approximation to h, found by using r_p, was used to determine $\bar{r}$. The correct heat-transfer area is then found using the $\bar{r}$ computed from equation (A13). The correction to the area of the plug is approximately 20 percent for the tests reported herein.

REFERENCES

1. Penland, Jim A.: Aerodynamic Characteristics of a Circular Cylinder at Mach Number 6.86 and Angles of Attack up to 90°. NACA RM L54A14, 1954.

2. King, Louis Vesset: On the Convection of Heat From Small Cylinders in a Stream of Fluid. Trans. Phil. Roy. Soc., London, ser. A., vol. 214, 1914, pp. 373-432.

3. Weske, John R.: Measurements of the Arithmetic Mean Velocity of a Pulsating Flow at High Velocity by the Hot-Wire Method. NACA TN 990, 1946.

4. Lowell, Herman H.: Design and Application of Hot-Wire Anemometers for Steady State Measurements at Transonic and Supersonic Airspeeds. NACA TN 2117, 1950.

5. Eggers, A. J., Jr., Hansen, C. Frederick, and Cunningham, Bernard E.: Theoretical and Experimental Investigation of the Effect of Yaw on Heat Transfer to Circular Cylinders in Hypersonic Flow. NACA RM A55E02, 1955.

6. Sears, W. R.: The Boundary Layer of Yawed Cylinders. Jour. Aero. Sci., vol. 15, no. 1, Jan. 1948, pp. 49-52.

7. Crabtree, L. F.: The Compressible Laminar Boundary Layer on a Yawed Infinite Wing. The Aeronautical Quarterly, vol. V, July 1954, pp. 85-100.

8. Howarth, Leslie: Modern Developments in Fluid Dynamics - High-Speed Flow. Vol. 2, Clarendon Press (Oxford), 1953, pp. 759-850.

9. Chapman, Dean R., and Rubesin, Morris W.: Temperature and Velocity Profiles in the Compressible Laminar Boundary Layer with Arbitrary Distribution of Surface Temperature. Jour. Aero. Sci., vol. 16, no. 9, Sept. 1949, pp. 547-565.

10. Reshotko, Eli, and Cohen, Clarence B.: Heat Transfer at the Forward Stagnation Point of Blunt Bodies. NACA TN 3513, 1955.

11. Stalder, Jackson R., Goodwin, Glen, and Creager, Marcus O.: A Comparison of Theory and Experiment for High-Speed Free-Molecule Flow. NACA Rep. 1032, 1951.

12. Owen, J. M., and Sherman, Frederick S.: Design and Testing of a Mach 4 Axially Symmetric Nozzle for Rarified Gas Flows. Rep. HE-150-104, Univ. of Calif., Institute of Engineering Research, July 23, 1952.

13. Stalder, Jackson R., Goodwin, Glen, and Creager, Marcus O.: Heat Transfer to Bodies in a High-Speed Rarified-Gas Stream. NACA Rep. 1093, 1952.

14. Walter, L. W., and Lange, A. H.: Surface Temperature and Pressure Distribution on a Circular Cylinder in Supersonic Cross-Flow. NAVORD Rep. 2854 (Aeroballistic Res. Rep. 180), U. S. Naval Ordnance Lab., White Oak, Md., June 5, 1953.

15. Cohen, Clarence B., and Reshotko, Eli: Similar Solutions for the Compressible Laminar Boundary Layer With Heat Transfer and Pressure Gradient. NACA TN 3325, 1954.

16. Feller, William V.: Investigation of Equilibrium Temperatures and Average Laminar Heat-Transfer Coefficients for the Front Half of Swept Circular Cylinders at $M = 6.9$. NACA RM L55F08, 1955.

17. von Kármán, Theodor, and Biot, Maurice A.: Mathematical Methods in Engineering. First ed., McGraw-Hill Book Company, New York, N. Y. 1940, p. 62.

TABLE I.- STREAM CONDITIONS

Static pressure, microns Hg abs	Mach number	Stream diameter, in.
320	3.90	3.6
180	3.90	3.0
110	3.75	3.0

TABLE II.- PRESSURE SURVEY DATA

Λ, deg	φ, deg	p_1, Hg abs	p_∞, micron Hg abs	M	R_2	R_∞
0	0	6.54	.319	3.94	1890	6.7×10^3
	15	6.18				
	30	5.17				
	45	3.80				
	60	2.48				
	75	1.43				
	90	.75				
	105	.42				
	120	.28				
	135	.24				
	150	.25				
	165	.26				
	180	.26				
30	0	5.05	.318	3.90	1890	6.7×10^3
	15	4.77				
	30	3.97				
	45	2.80				
	60	1.85				
	75	1.08				
	90	.60				
45	0	1.05	.10	3.8	610	2.1×10^3
	15	1.00				
	30	.85				
	45	.66				
	60	.46				
	75	.29				
	90	.18				

TABLE III.- TEST DATA

Λ, deg	φ, deg	h, $\frac{\text{Btu}}{\text{hr ft}^2\ {}^\circ\text{F}}$	S, 10^{-4} ft^2	T_r, $^\circ$R	T_t, $^\circ$R	M	p_∞, microns Hg abs	R_2	R_∞
0	0	9.05	1.012	532	534	3.94	306	1890	6.7×10^3
	15	8.78	1.013	532	534				
	30	7.86	1.018	526	532				
	45	6.46	1.025	519	532				
	60	4.62	1.032	504	532				
	75	3.21	1.040	489	535				
	90	1.83	1.059	459	537				
	105	1.14	1.066	441	537				
	120	.69	1.070	402	534				
	135	.63	1.070	438	533				
	150	.44	1.075	498	534				
	165	.47	1.072	534	534				
	180	.58	1.070	534	534				
	0	4.42	1.025	526	529	3.80	105	610	2.1×10^3
	15	4.63	1.024	526	529				
	30	3.86	1.030	525	535				
	45	3.41	1.033	520	535				
	60	2.52	1.042	509	535				
	75	1.68	1.052	472	529				
	90	1.22	1.040	467	529				
	0	7.77	1.010	524	523	3.90	180	1120	3.8×10^3
	15	7.51	1.012	525	525				
	30	6.50	1.017	521	526				
	45	5.24	1.024	506	525				
	60	3.85	1.035	500	527				
	75	2.57	1.047	480	528				
	90	1.56	1.058	457	528				
30	0	7.86	1.019	519	532	3.91	300	1890	6.3×10^3
	15	7.59	1.018	519	532				
	30	6.82	1.023	511	527				
	45	5.44	1.031	503	527				
	60	3.43	1.045	495	531				
	75	2.39	1.053	473	533				
	90	1.24	1.064	434	533				
44	0	6.43	1.026	509	530	3.91	320	1890	6.7×10^3
	15	6.12	1.028	506	530				
	30	4.75	1.036	489	522				
	45	3.97	1.042	474	522				
	60	2.75	1.051	467	523				
	75	1.96	1.058	453	525				
	90	1.45	1.063	460	530				

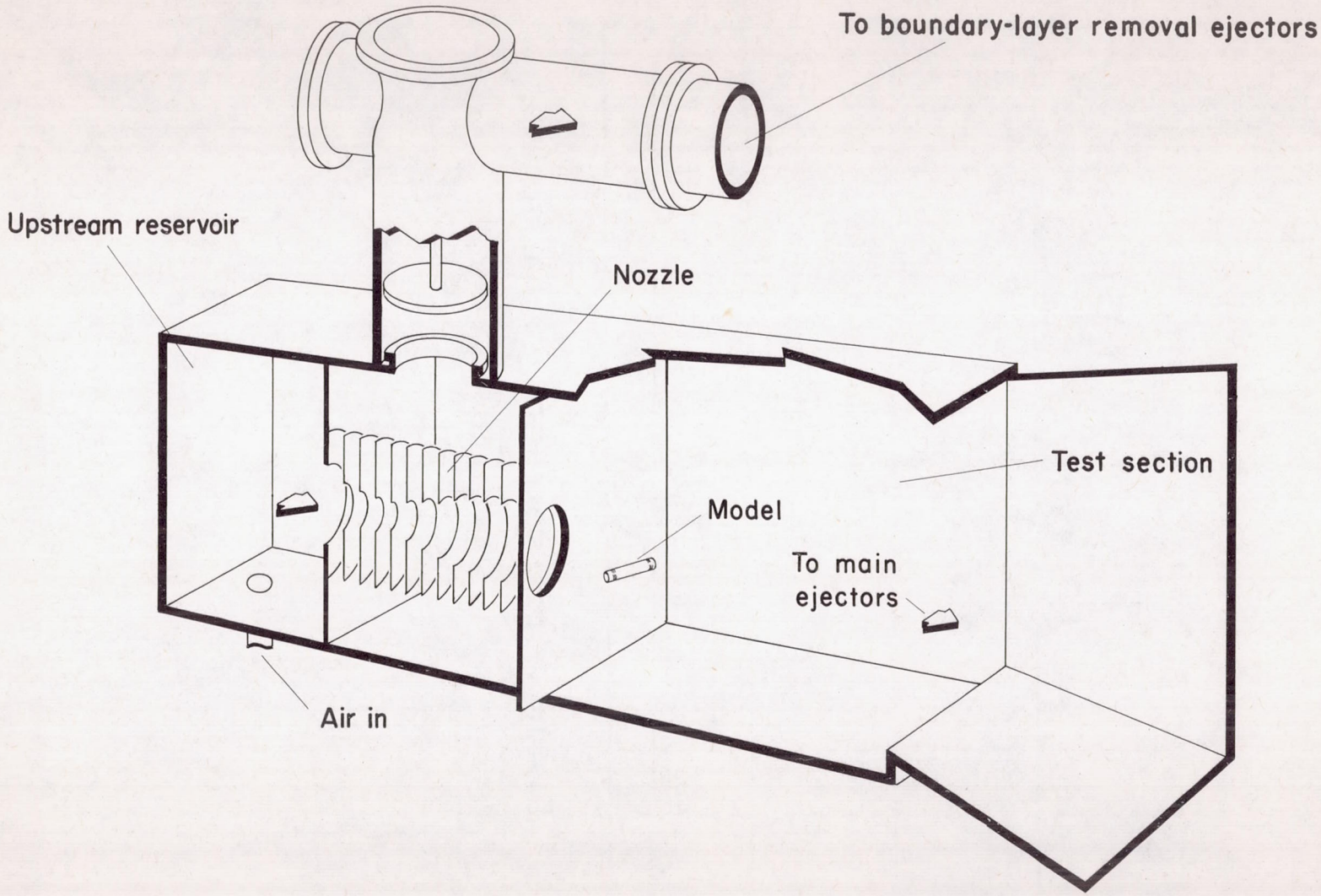

Figure 1. - General arrangement of wind-tunnel test section, nozzle, and model.

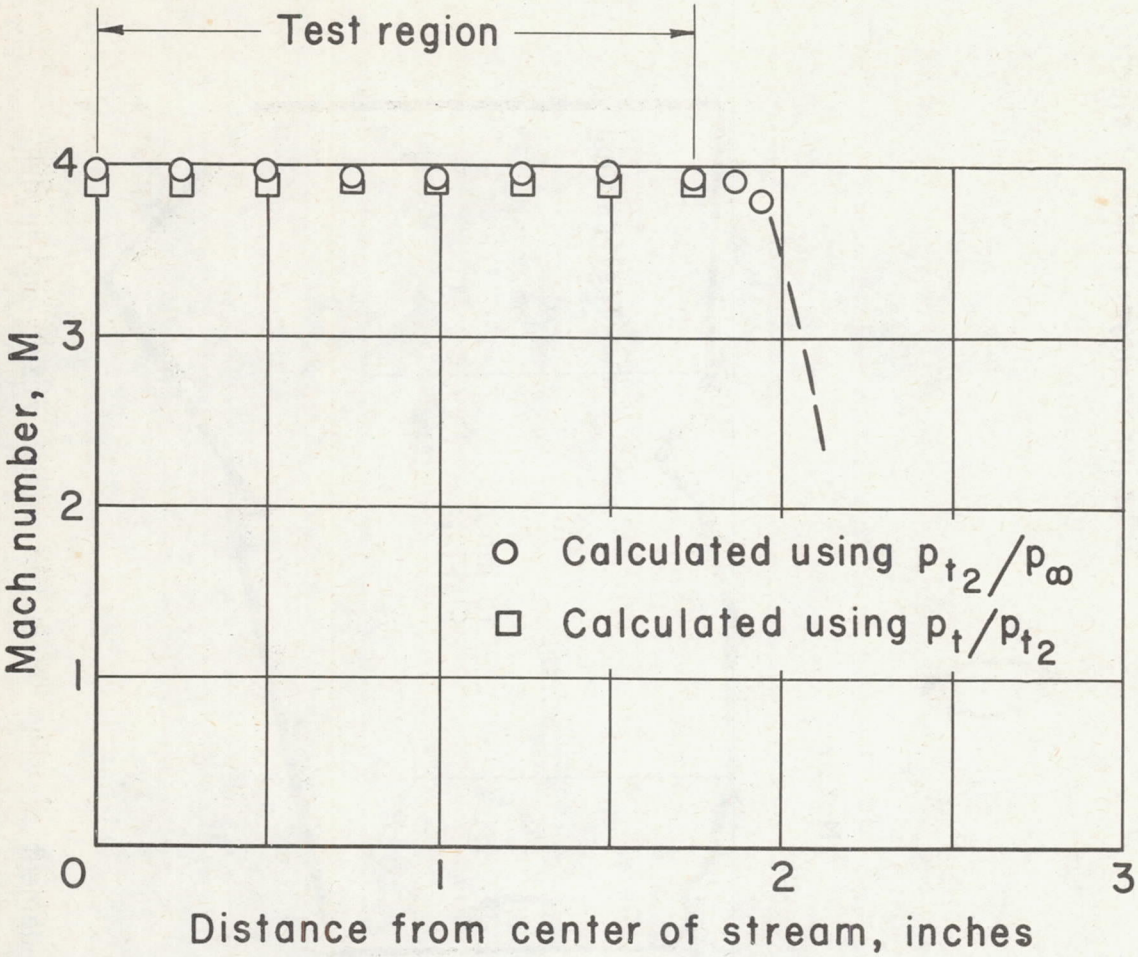

Figure 2.- Variation of Mach number with distance from center of stream for Reynolds number per foot of 8.7×10^4 at axial distance of 1.25 inches from exit plane of nozzle.

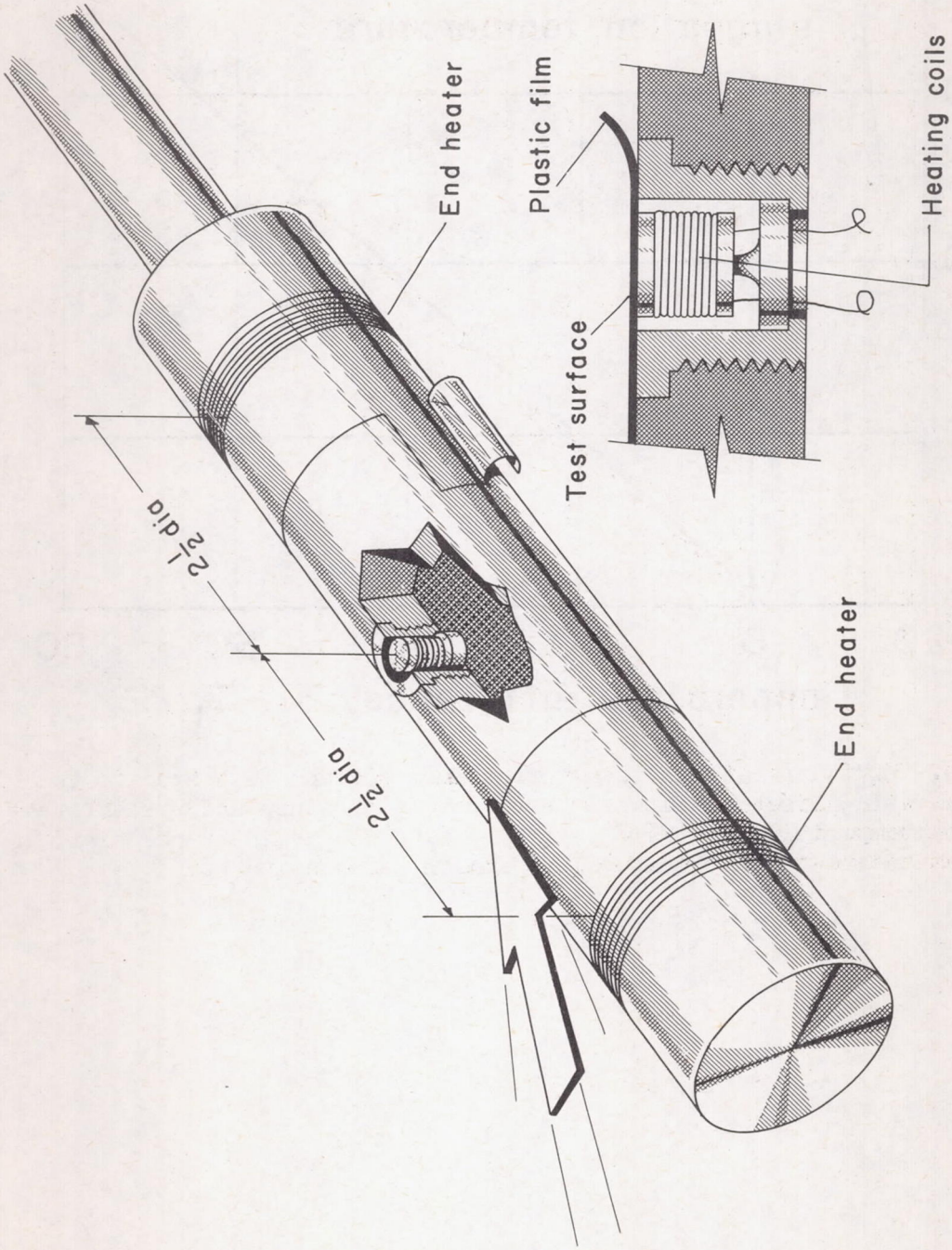

Figure 3.- Test model.

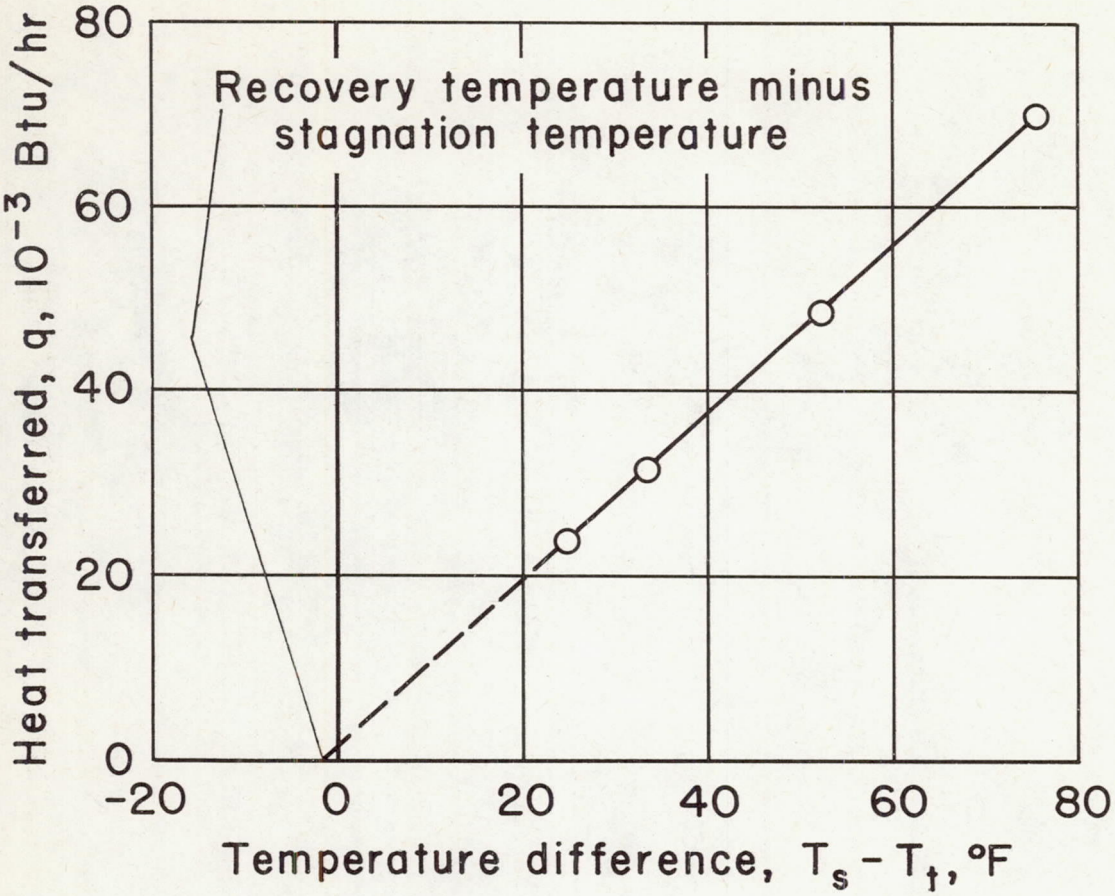

Figure 4.- Variation of heat transferred from surface test area to the stream with difference between test area temperature and stream stagnation temperature for $M = 3.94$; $R_\infty = 6.7 \times 10^3$, cylinder normal to stream and test area oriented 15° from the stagnation point.

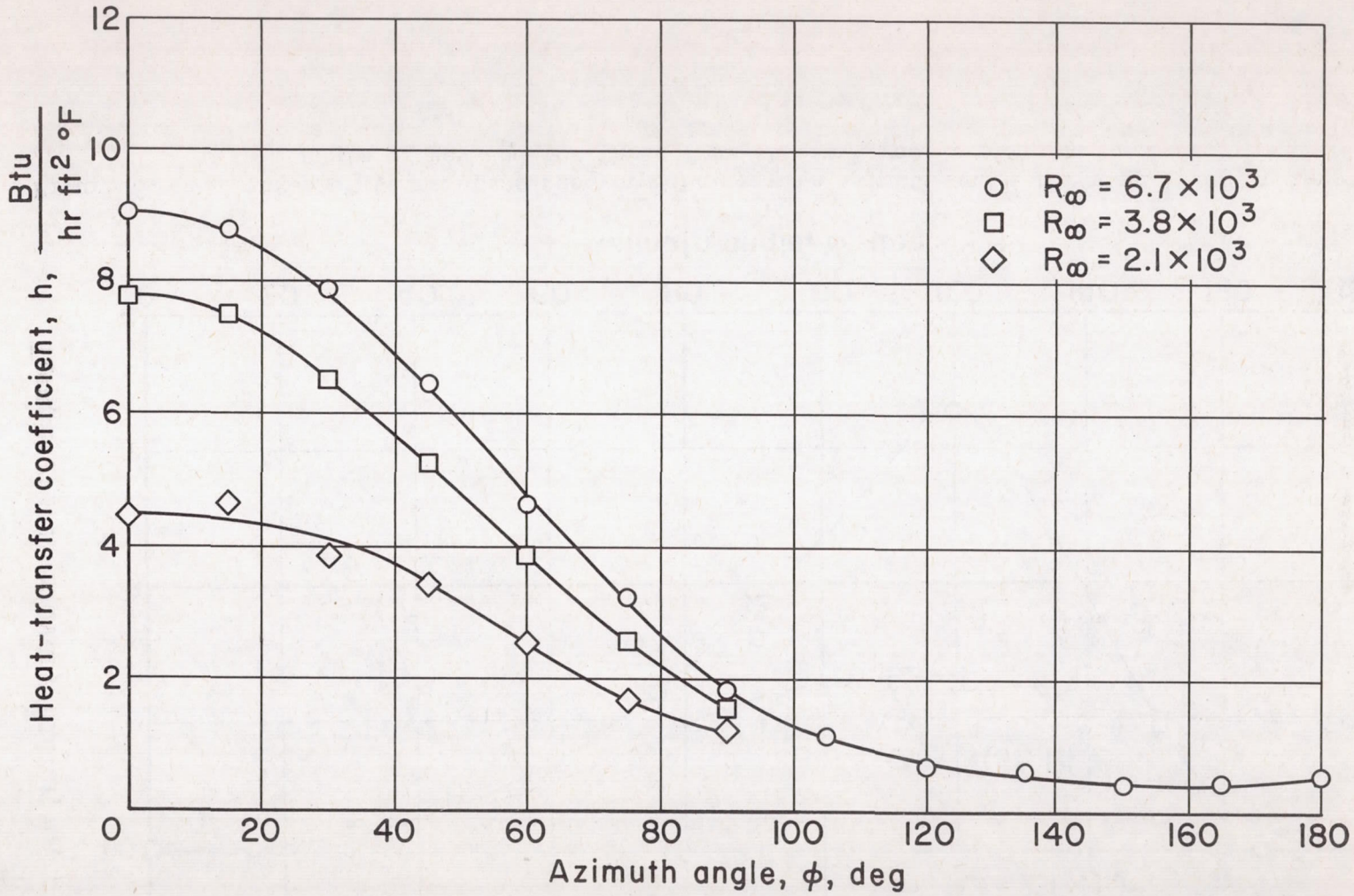

Figure 5.- Variation of local heat-transfer coefficient with azimuth angle for a cylinder at zero angle of yaw and for three free-stream Reynolds numbers.

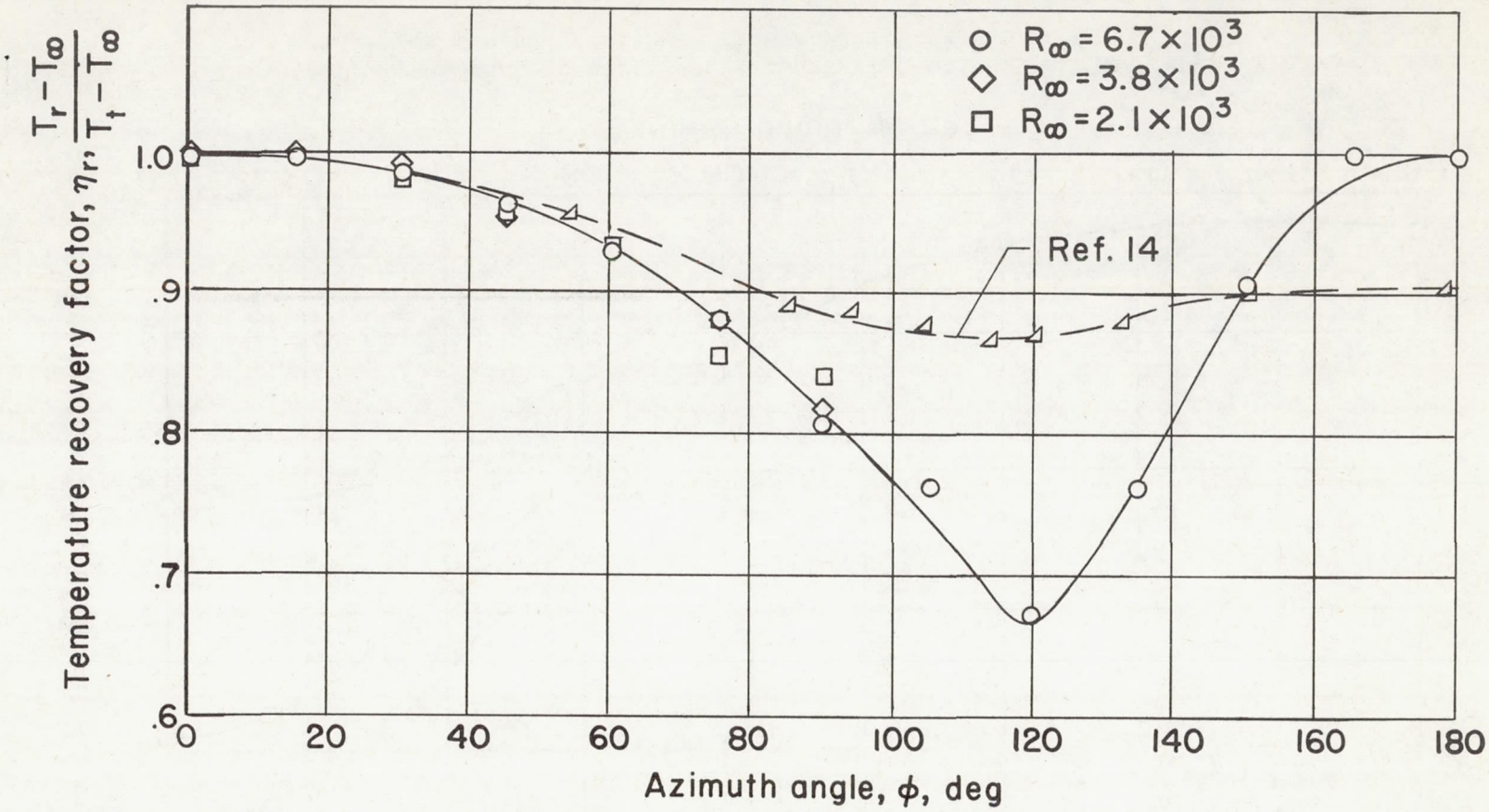

Figure 6.- Variation of temperature recovery factor with azimuth angle for a cylinder at zero angle of yaw and for three free-stream Reynolds numbers.

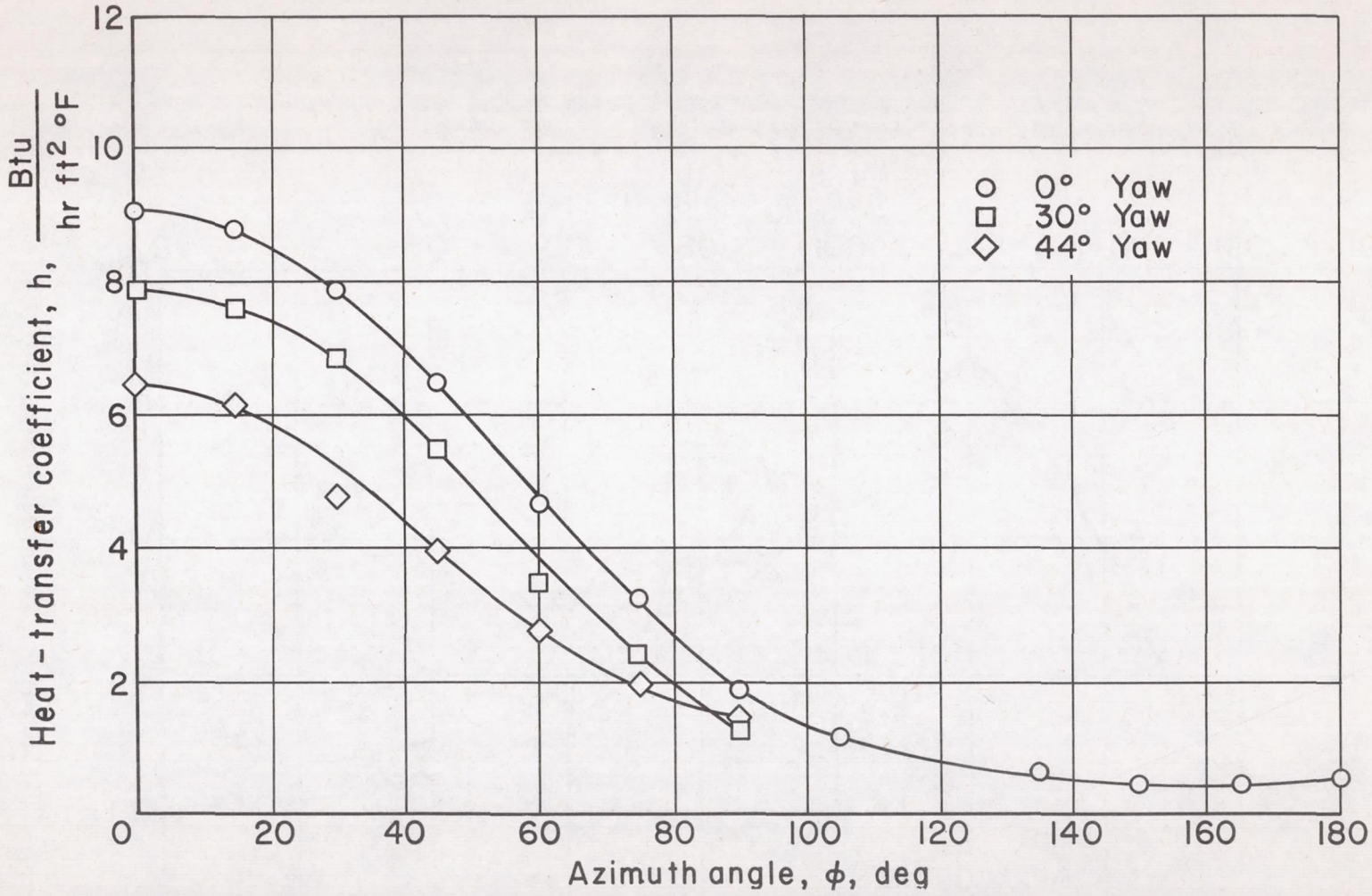

Figure 7.- Variation of local heat-transfer coefficient with azimuth angle for a cylinder at various angles of yaw, for a free-stream Reynolds number of 6.7×10^3.

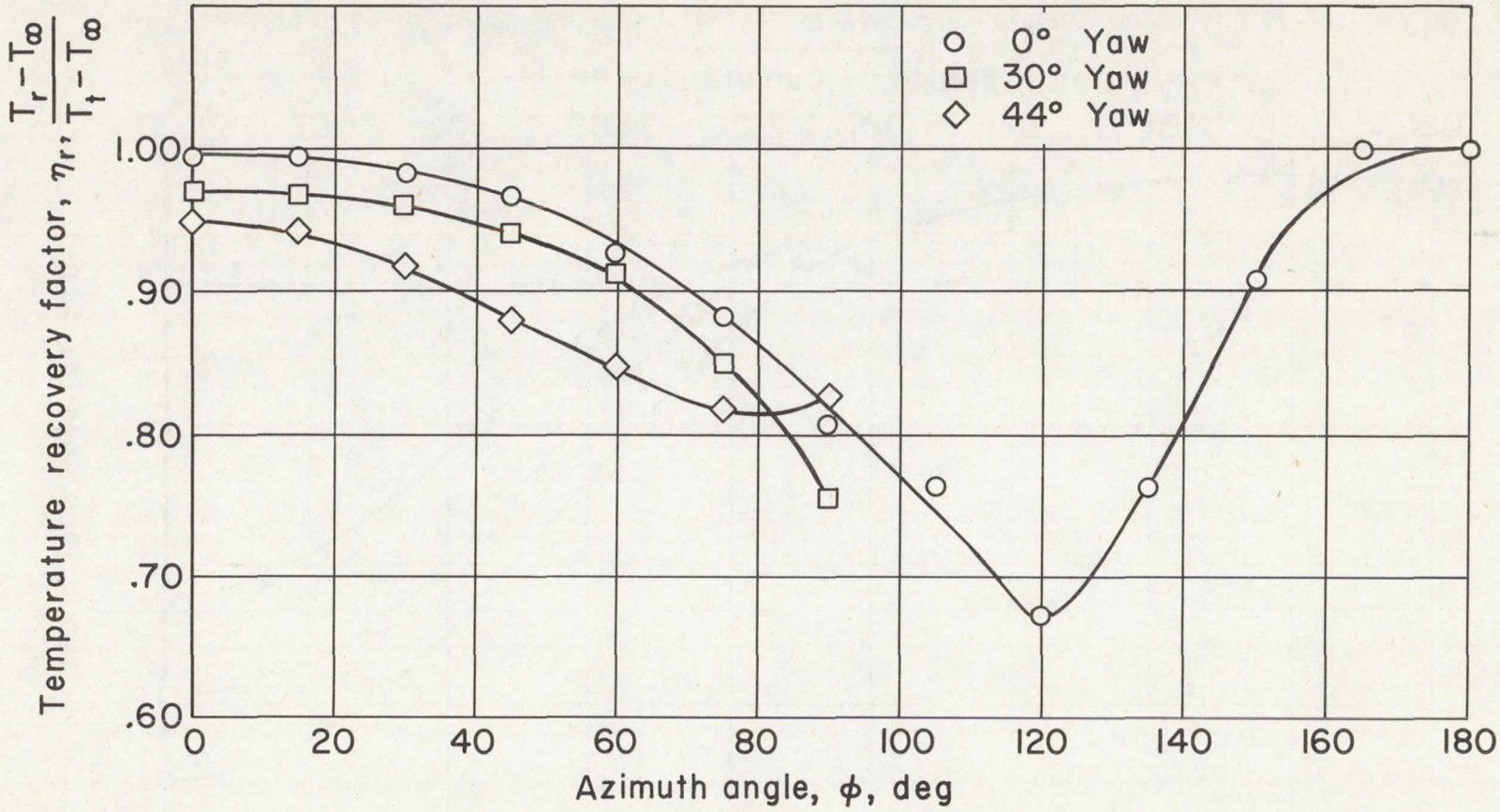

Figure 8.- Variation of temperature recovery factor with azimuth angle for a cylinder at various angles of yaw for a free-stream Reynolds number of 6.7×10^3.

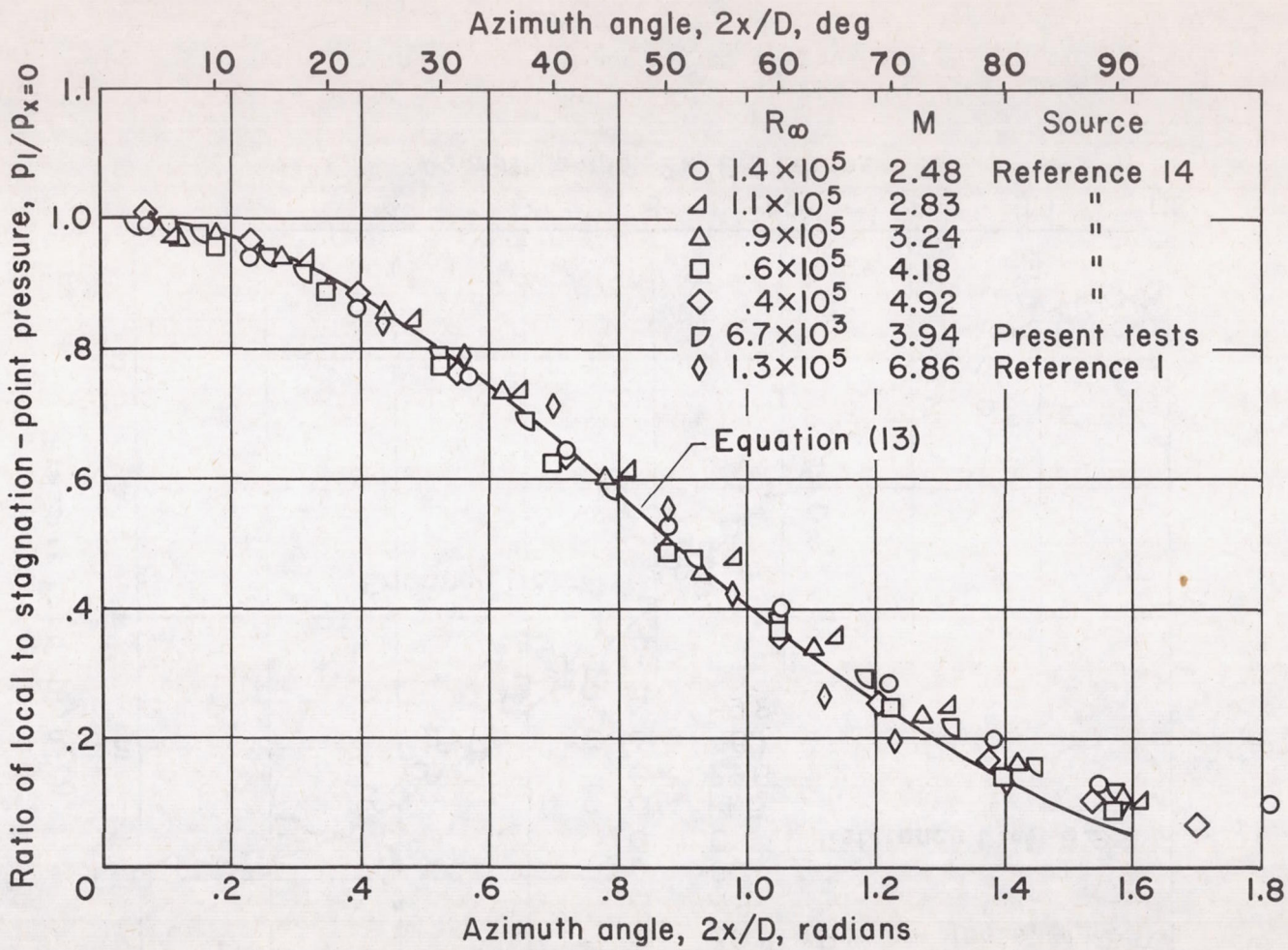

Figure 9.- Variation of the ratio of local to stagnation-point pressure with azimuth angle for a cylinder at zero angle of yaw.

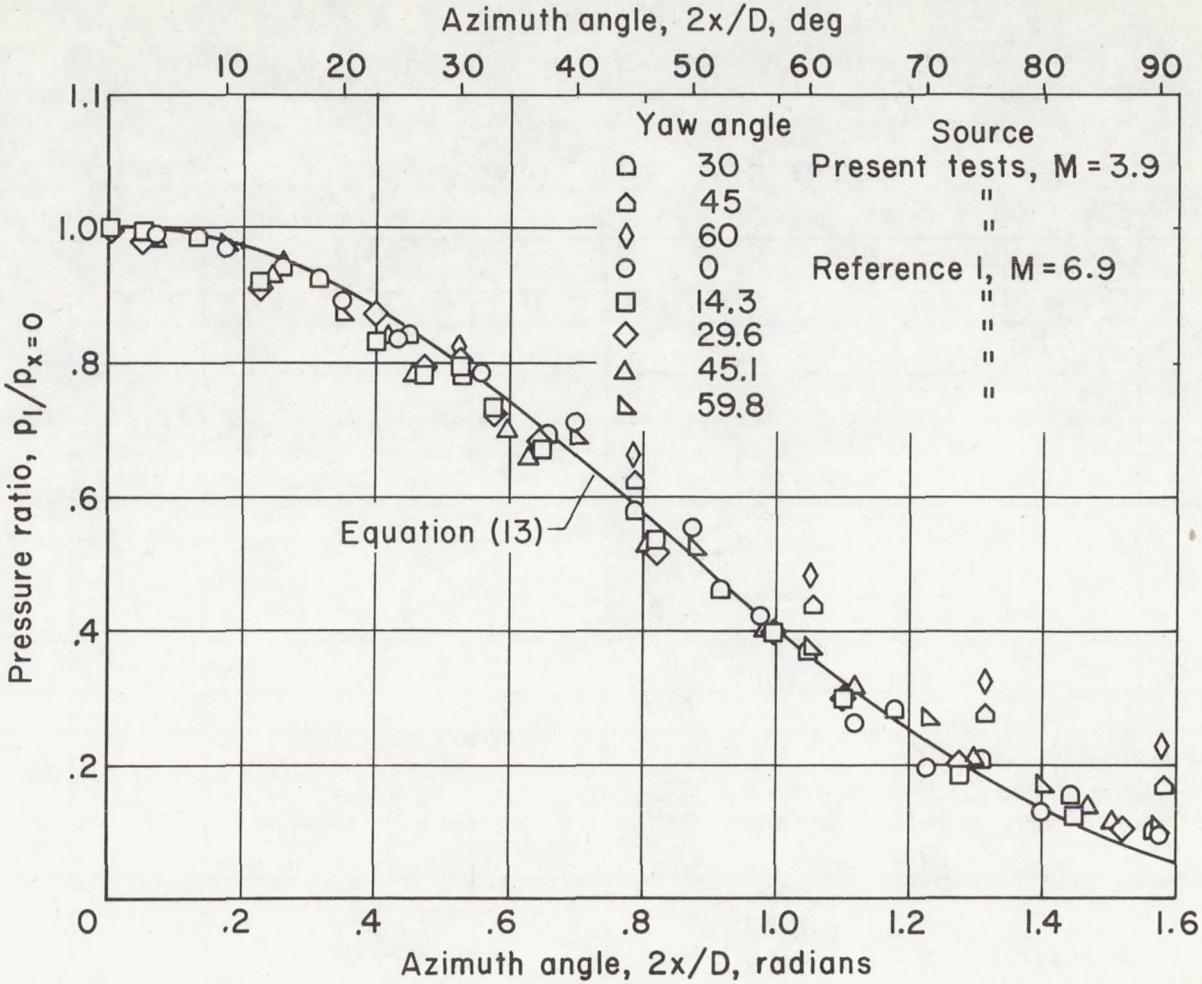

Figure 10.- Variation of the ratio of local pressure to the pressure at $x = 0$ with azimuth angle for a cylinder at various angles of yaw.

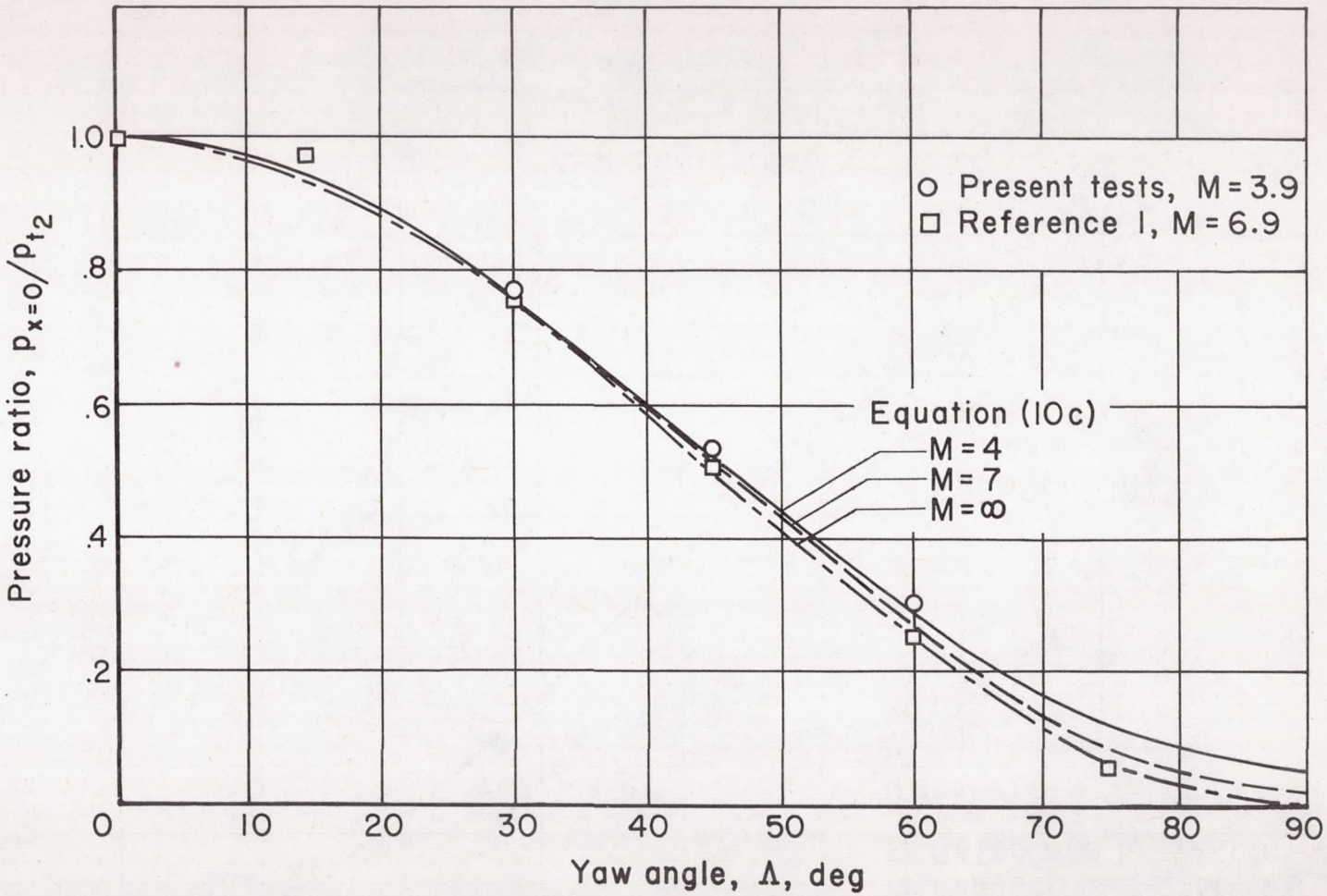

Figure 11.- Variation of ratio of pressure at $x = 0$ to stream impact pressure with angle of yaw of a cylinder.

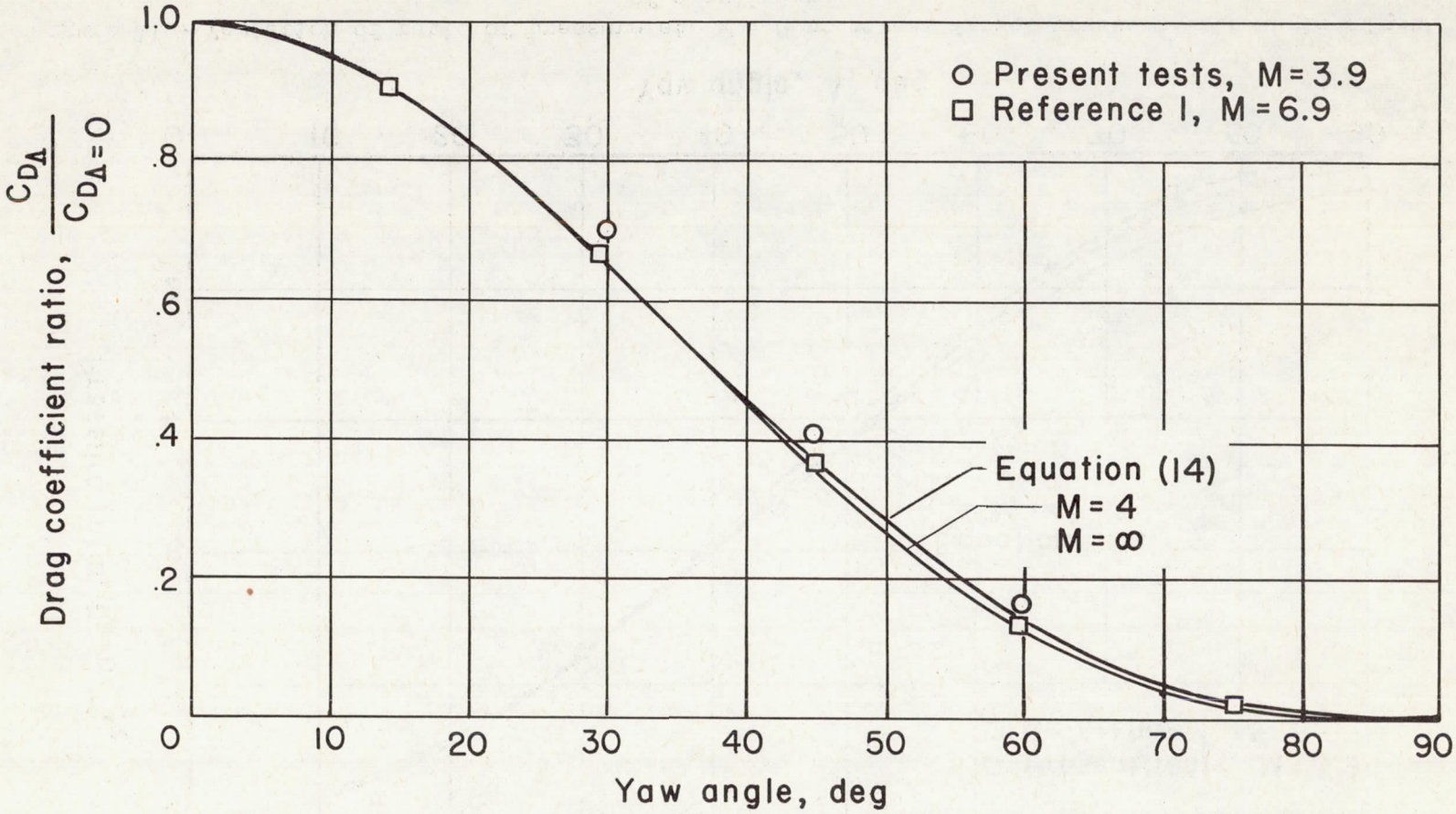

Figure 12.- Variation of ratio of pressure drag coefficient for front side of yawed to unyawed cylinders with angle of yaw.

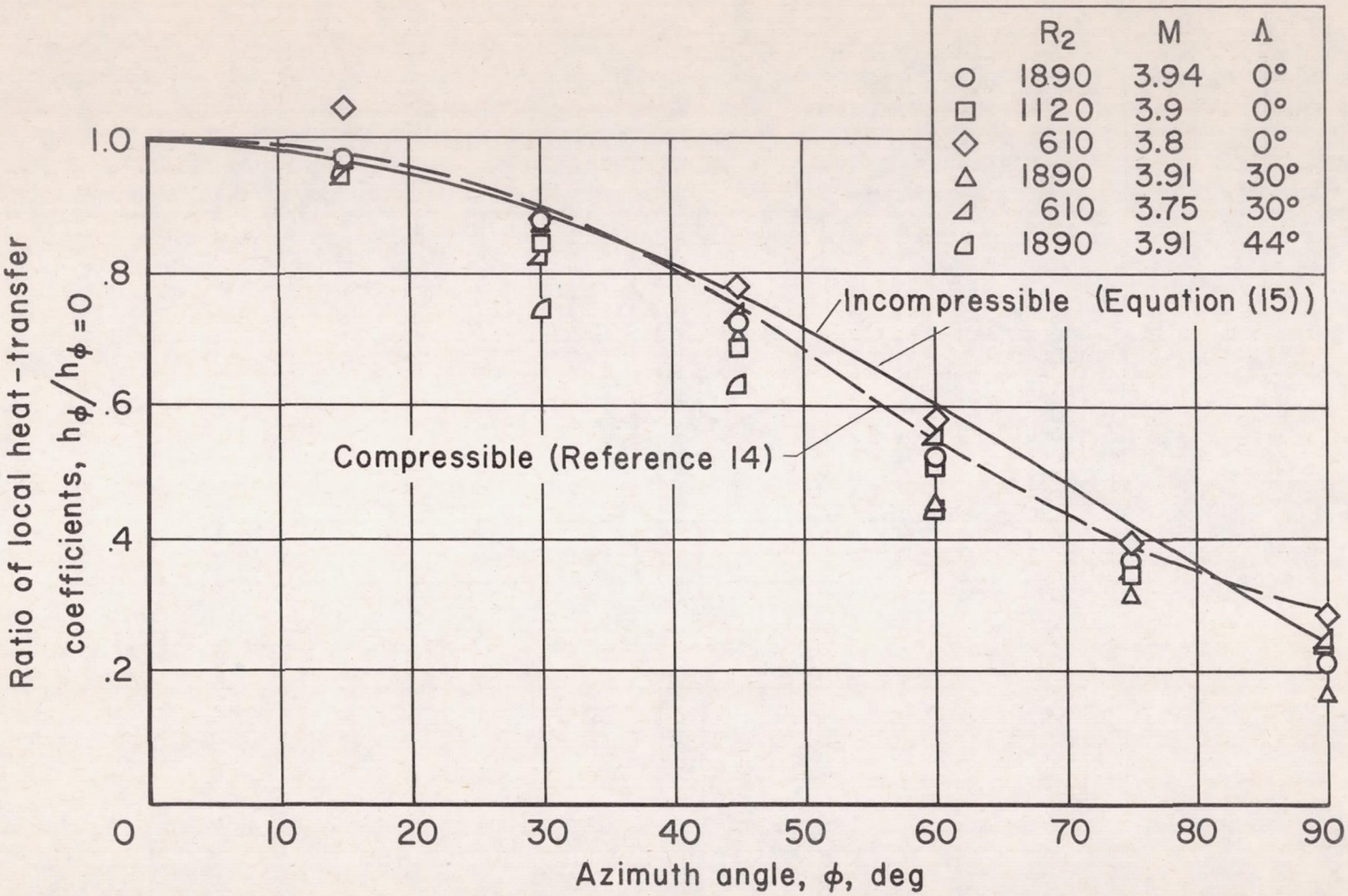

Figure 13.- Theoretical and experimental variation of the ratio of the local heat-transfer coefficient to heat-transfer coefficient at $\varphi = 0$ with azimuth angle for various angles of yaw and Reynolds numbers.

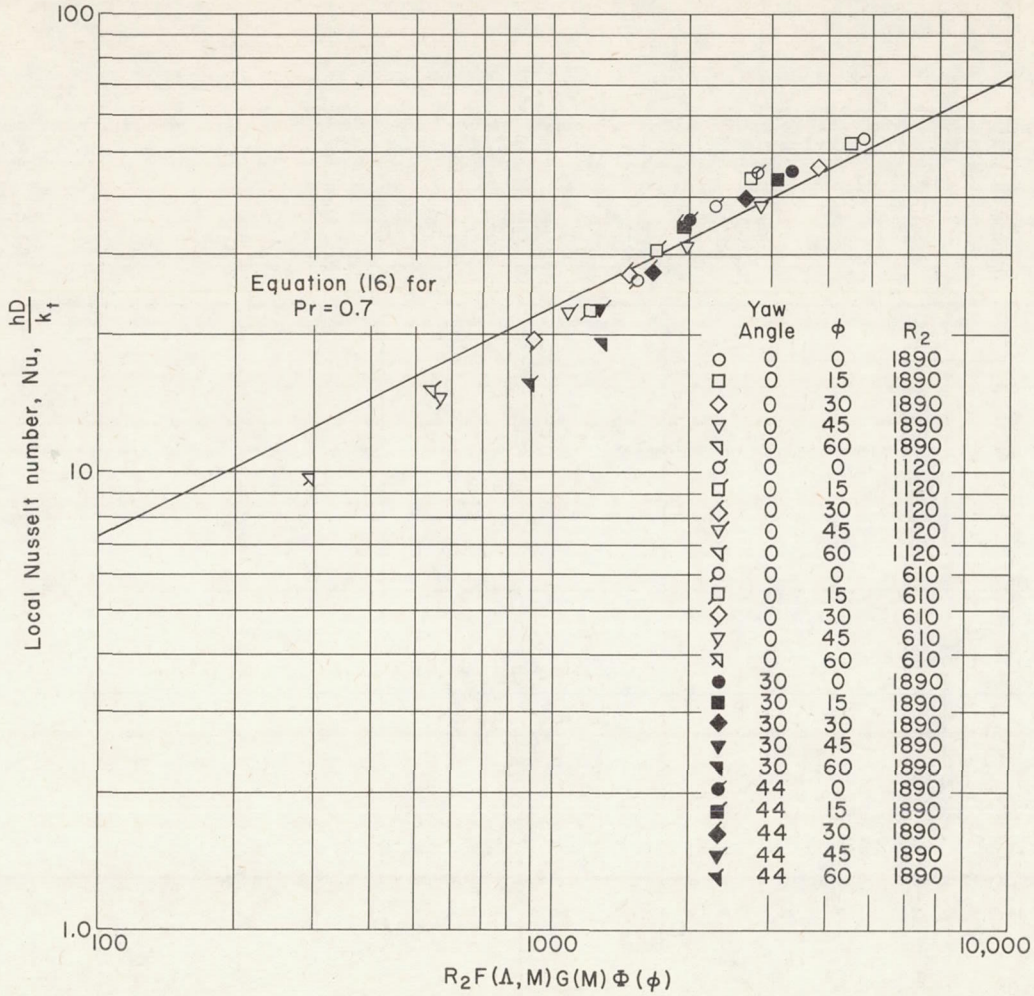

Figure 14.- Comparison of experimental and theoretical variation of local Nusselt number with the quantity $R_2F(\Lambda,M)G(M)\Phi(\varphi)$ for various angles of yaw, azimuth angles, and Reynolds numbers.

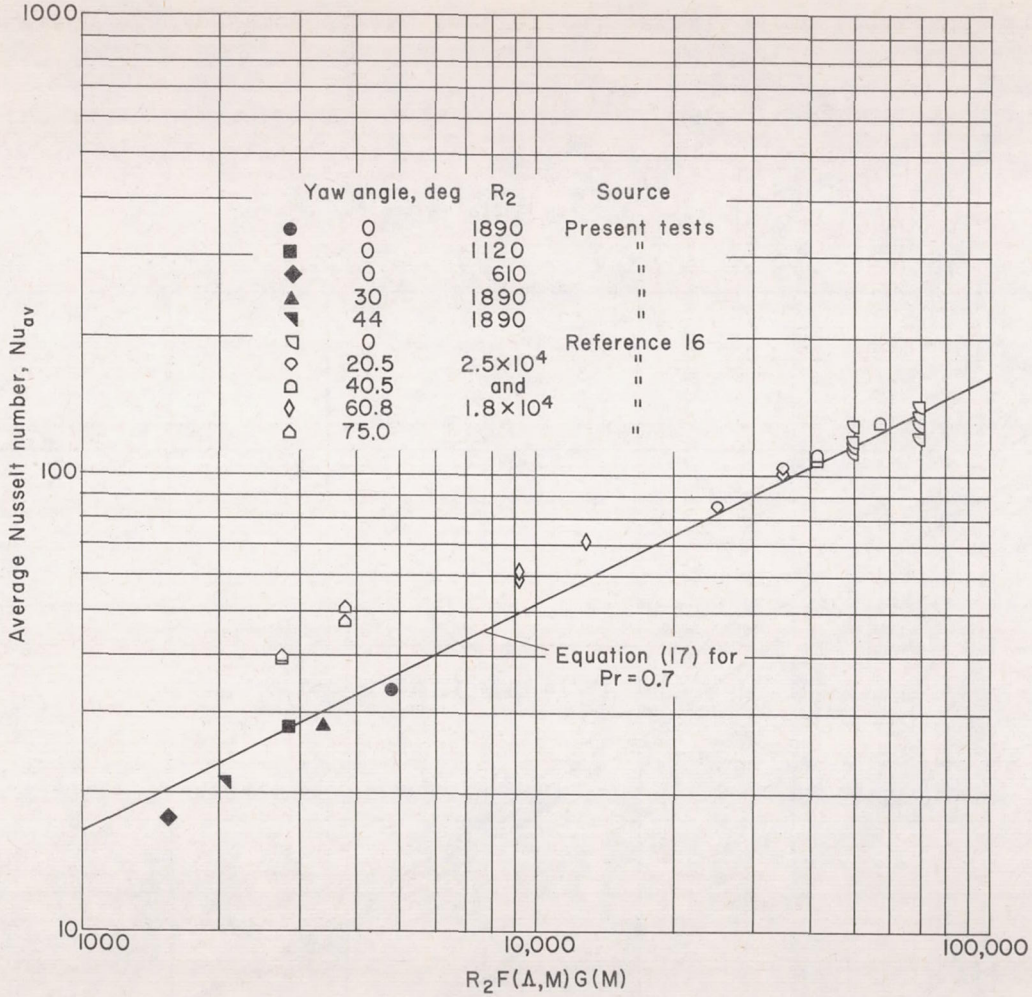

Figure 15.- Comparison of experimental and predicted variation of Nusselt number, averaged over the front half of the cylinder, with the quantity $R_2F(\Lambda,M)G(M)$.

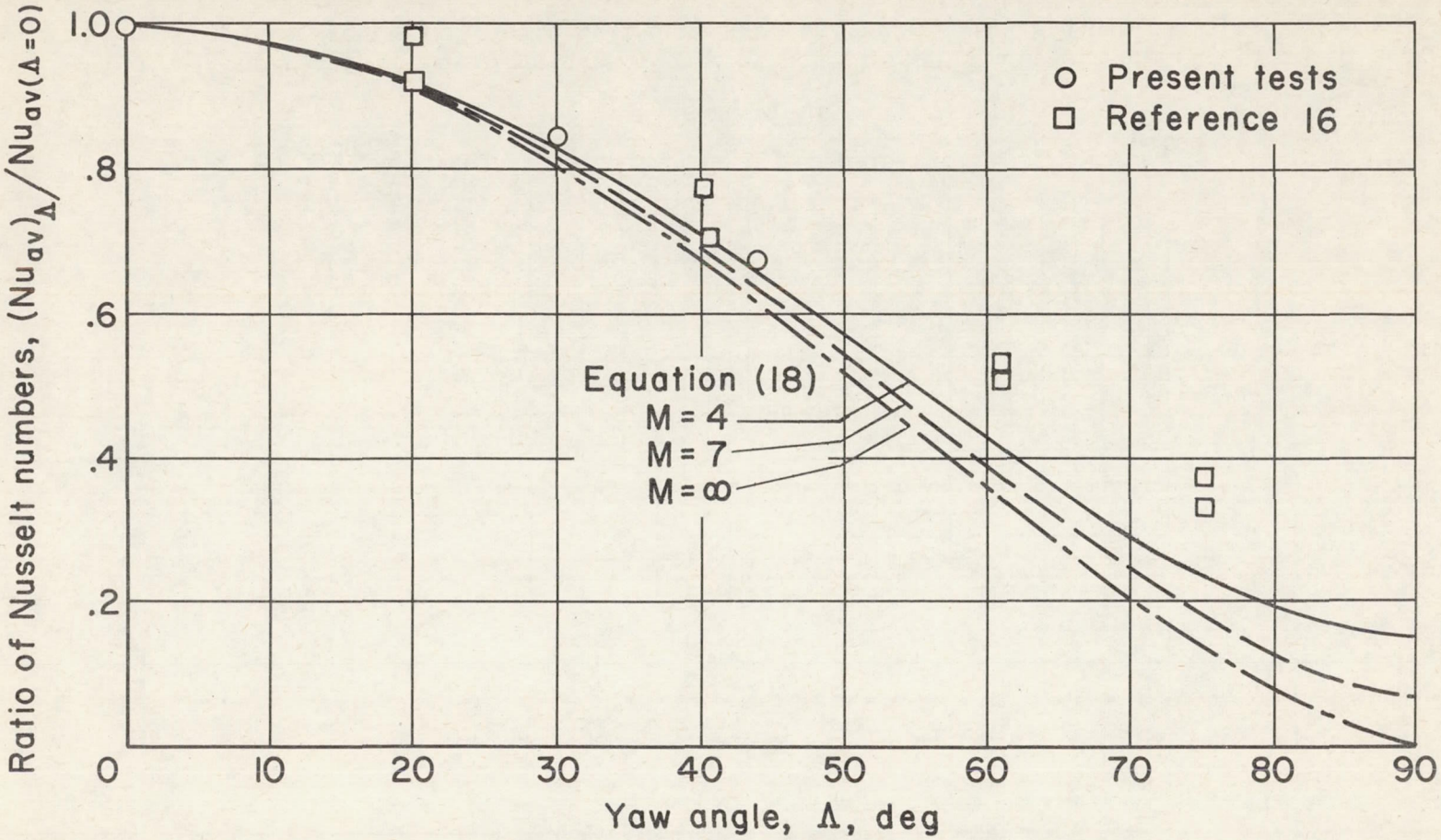

Figure 16.- Comparison of experimental and predicted variation of ratio of the average Nusselt number for yawed cylinders to average Nusselt number of cylinder at zero yaw.

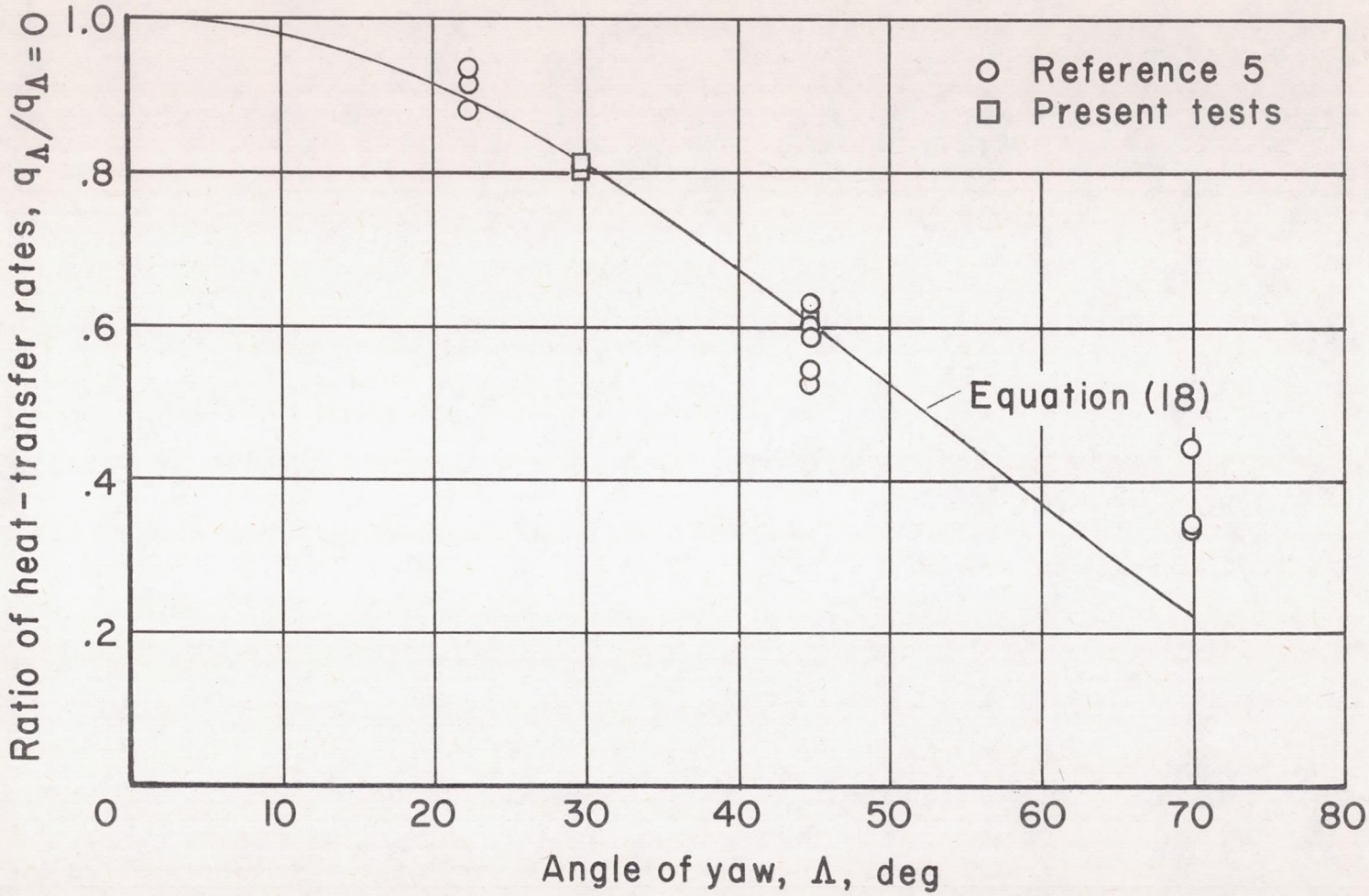

Figure 17.- Comparison of experimental and predicted variation of the ratio of total heat transferred from front side of cylinder with angle of yaw; $M = 9.8$, $T_t = 2200^\circ$ R. Data from reference 5 include heat transferred from back side of cylinder.

NACA - Langley Field, Va.